0013-7227/05/$15.00/0
Printed in U.S.A.

Endocrinology 146(5):2255–2264
Copyright © 2005 by The Endocrine Society
doi: 10.1210/en.2004-0695

Ingested Medium-Chain Fatty Acids Are Directly Utilized for the Acyl Modification of Ghrelin

Yoshihiro Nishi, Hiroshi Hiejima, Hiroshi Hosoda, Hiroyuki Kaiya, Kenji Mori, Yoshihiko Fukue, Toshihiko Yanase, Hajime Nawata, Kenji Kangawa, and Masayasu Kojima

Department of Molecular Genetics (Y.N., H.Hi., Y.F., M.K.), Institute of Life Science, Kurume University, Kurume, Fukuoka 839-0861; Department of Biochemistry (H.Ho., H.K., K.M., K.K), National Cardiovascular Center Research Institute, Osaka 565-8565; and Department of Bioregulatory Science (T.Y., H.N.), Graduate School of Medical Science, Kyushu University, Fukuoka 812-8582, Japan

Ghrelin, an acylated brain and gut peptide, is primarily produced by endocrine cells of the gastric mucosa for secretion into the circulation. The major active form of ghrelin is a 28-amino-acid peptide containing an *n*-octanoyl modification at serine that is essential for activity. Studies have identified multiple physiological functions for ghrelin, including GH release, appetite stimulation, and metabolic fuel preference. Until now, there has not been any report detailing the mechanism of ghrelin acyl modification. Here we report that ingestion of either medium-chain fatty acids (MCFAs) or medium-chain triacylglycerols (MCTs) increased the stomach concentrations of acylated ghrelin without changing the total (acyl- and des-acyl-) ghrelin amounts. After ingestion of either MCFAs or MCTs, the carbon chain lengths of the acyl groups attached to nascent ghrelin molecules corresponded to that of the ingested MCFAs or MCTs. Ghrelin peptides modified with *n*-butyryl or *n*-palmitoyl groups, however, could not be detected after ingestion of the corresponding short-chain or long-chain fatty acids, respectively. Moreover, *n*-heptanoyl ghrelin, an unnatural form of ghrelin, could be detected in the stomach of mice after ingestion of either *n*-heptanoic acid or glyceryl triheptanoate. These findings indicate that ingested medium-chain fatty acids are directly used for the acylation of ghrelin. (*Endocrinology* 146: 2255–2264, 2005)

GHRELIN WAS DISCOVERED by our group as an endogenous ligand for the receptor for GH secretagogues, synthetic and unnatural substances with potent GH-releasing activities (1). Whereas initially purified from the stomach, ghrelin is also expressed within the brain, lung, kidney, pancreas, small intestine, and large intestine (2–7). In addition to potent GH-releasing activity (1, 8–10), ghrelin also stimulates appetite, induces adiposity (11–14), improves cardiac function (15–17), and influences metabolic fuel preference (18).

The third amino acid residue of ghrelin, serine (Ser^3), is modified by an acyl group; this modification is essential for ghrelin biological activity (1). Whereas the primary acyl chain-modifying ghrelin molecules in humans and rodents are an *n*-octanoyl group (C8:0, an eight-carbon chain containing no double bonds) (1, 19), additional acyl modifications create a minor population of ghrelin peptides. These acyl groups include *n*-decanoyl (C10:0, a 10-carbon chain lacking double bonds) and *n*-decanoyl (C10:1, a 10-carbon chain containing one double bond) (20–22). Our examination of a variety of synthetic acyl-modified ghrelin peptides determined that the potency of ghrelin biological activity was altered by different modifying acyl groups (23).

To our knowledge, the acyl modification of ghrelin is the first example of the fatty acid modification of a peptide hormone; acylation of a serine hydroxyl group has not been previously reported as a mammalian peptide hormone modification. The enzyme catalyzing the transfer of acyl groups to ghrelin Ser^3, likely a novel acyltransferase, will be important in the regulation of ghrelin production. The nature of this enzyme, however, remains unknown.

We report here that ingested medium-chain fatty acids (MCFAs) and medium-chain triglycerides serve as a source of fatty acids in the acyl modification of ghrelin. Ingestion of MCFAs (*n*-hexanoic, *n*-octanoic, and *n*-decanoic acid) or medium-chain triglycerides (glyceryl trihexanoate, glyceryl trioctanoate, and glyceryl tridecanoate) increased the stomach concentrations of ghrelin bearing an acyl group with the corresponding carbon chain length, *i.e.* *n*-hexanoyl ghrelin, *n*-octanoyl ghrelin, and *n*-decanoyl ghrelin. Ingestion of such lipids, however, did not significantly alter total ghrelin (acyl-modified and des-acyl ghrelin with an intact C-terminal peptide sequence) production. Ingestion by mice of glyceryl triheptanoate, which cannot be naturally synthesized by mammalian cells, resulted in the production of an unnatural ghrelin form incorporating an *n*-heptanoyl modification. These findings indicate that ingested MCFAs and medium-chain triglycerides are likely the direct source of fatty acids destined for acyl modification of ghrelin.

First Published Online January 27, 2005

Abbreviations: AcOH, Acetic acid; $[Ca^{2+}]_i$, intracellular-free calcium concentration; CH_3CN, acetonitrile; C-RIA, radioimmunoassay to C-terminal fragment of ghrelin(13–28); C18 RP-HPLC, reverse-phase HPLC with C18-cartridge; FFA, free fatty acid; GHS-R, GH ghrelin receptor; HF, high-fat (diet); LCT, long-chain triglyceride; -LI, -like immunoreactivity; MALDI-TOF-MS, matrix-assisted laser desorption/ionization time-of-flight mass spectrometry; MCFA, medium-chain fatty acid; MCT, medium-chain triglyceride; N-RIA, radioimmunoassay to N-terminal fragment of *n*-octanoyl ghrelin(1–11); Ser^3, serine; TFA, trifluoroacetic acid.

Endocrinology is published monthly by The Endocrine Society (http://www.endo-society.org), the foremost professional society serving the endocrine community.

Downloaded from endo.endojournals.org on March 19, 2006

Materials and Methods

Animals

Male C57BL/6J mice weighing 20–25 g were used in these experiments. Animals were maintained under controlled temperature (21–23 C) and light conditions (light on 0700–1900 h) with *ad libitum* access to food and water. All experiments were conducted in accordance with the Kurume University Guide for the Care and Use of Experimental Animals.

RIA of ghrelin

RIAs specific for ghrelin were performed as previously described (2). Rabbit polyclonal antibodies were raised against the N terminal [(Gly^1-Lys^{11}) with *O*-*n*-octanoylation at Ser^3] and C-terminal (Gln^{13}-Arg^{28}) fragments of rat ghrelin. RIA incubation mixtures contained 100 μl of either standard ghrelin or an unknown sample with 200 μl of antiserum diluted in RIA buffer [50 mM sodium phosphate buffer (pH 7.4), 0.5% BSA, 0.5% Triton X-100, 80 mM NaCl, 25 mM EDTA-2Na, and 0.05% NaN_3] containing 0.5% normal rabbit serum. Antirat ghrelin (1–11) and antirat ghrelin(13–28) antisera were used at final dilutions of 1:3 million and 1:20,000, respectively. After a 12-h incubation at 4 C, 100 μl ^{125}I-labeled ligand (20,000 cpm) was added for an additional 36-h incubation. Then samples were incubated for 24 h at 4 C with 100 μl of antirabbit goat antibody. Free and bound tracers were then separated by centrifugation at 3000 rpm for 30 min. Pellet radioactivity was quantified in a γ-counter (ARC-600, Aloka, Tokyo, Japan). All assays were performed in duplicate.

Both antisera exhibited complete cross-reactivity with human, mouse, and rat ghrelin forms (2). The antirat ghrelin(1–11) antiserum, which specifically recognizes the *n*-octanoylated portion of ghrelin, exhibited 100% cross-reactivity with rat, mouse, and human *n*-octanoyl ghrelin but does not recognize des-acyl ghrelin. The cross-reactivity of N-terminal RIA for *n*-decanoyl and *n*-decanoyl ghrelin was approximately 20 and 25%, respectively. Cross-reactivity to *n*-butyryl, *n*-hexanoyl, *n*-lauryl, and *n*-palmitoyl ghrelin was less than 5%. Antirat ghrelin(13–28) antiserum equally recognizes both des-acyl and all acylated forms of ghrelin peptide including *n*-octanoyl, *n*-decanoyl, or *n*-decanoyl ghrelin (2). The ED_{50} for ghrelin C-terminal and N-terminal RIAs were approximately 32 and 8 fmol/tube, respectively. The minimal detection levels by C-terminal and N-terminal RIAs were 1.0 and 0.25 fmol/tube, respectively. The intraassay coefficients of variation of C-terminal and N-terminal RIAs were 6.0 and 3.0%, respectively. The interassay coefficients of variation were 7.0 and 5.0%, respectively. All samples measured by ghrelin assay were diluted in RIA buffer to fit the range of measurement (between ED_{20} to ED_{80}) for each RIA. Throughout the following sections, the RIA system using the antiserum raised against the N-terminal fragment of rat ghrelin(1–11) is termed N-RIA, whereas the RIA system using the antiserum recognizing the C-terminal fragment(13–28) is termed C-RIA. Ghrelin-like immunoreactivity (-LI) measured by C-RIA is termed ghrelin C-LI, whereas that measured by ghrelin N-RIA is termed ghrelin N-LI.

Calcium mobilization assays of ghrelin

CHO-GHSR62 cells (1) stably expressing rat ghrelin receptor (GHS-R) were plated for 12–15 h in flat-bottom black-walled 96-well plates (Corning Costar Corp., Cambridge, MA) at 4×10^4 cells/well. Cells were then preincubated for 1 h with 4 μM Fluo-4-AM fluorescent indicator dye (Molecular Probes, Inc., Eugene, OR) dissolved in assay buffer [Hanks' balanced salts solution, 10 mM HEPES, and 2.5 mM probenecid] supplemented with 1% fetal calf serum. After washing four times in assay buffer, samples were dissolved in 100 μl assay buffer with 0.01% BSA and added to the prepared cells. We then measured intracellular calcium concentration changes using a FLEX station (Molecular Devices, Sunnyvale, CA).

Preparation of stomach samples for ghrelin assay

All stomach samples, with the exception of those obtained at the 0 h point in the time-course study, were collected during a fed state. After collection from mice, stomachs were washed twice in PBS (pH 7.4). After measuring the wet weight of each sample, whole stomach tissue was diced and boiled for 5 min in a 10-fold volume of water to inactivate intrinsic proteases. After cooling, boiled samples were adjusted to 1 M acetic acid (AcOH)/20 mM HCl. After homogenization with a polytron mixer (PT 6100, Kinematica AG, Littan-Luzern, Switzerland), peptides were extracted and isolated by a 15-min centrifugation at 15,000 rpm (12,000 × *g*), were lyophilized and stored at −80 C. Lyophilized samples were redissolved in either RIA buffer or calcium mobilization assay buffer before ghrelin RIA or calcium mobilization assay, respectively.

Preparation of plasma samples for ghrelin assay

Plasma samples were prepared as previously described (2). Whole blood samples from 10 male mice were immediately transferred to chilled polypropylene tubes containing EDTA-2Na (1 mg/ml) and aprotinin (1000 kallikrein inactivator units per milliliter) and centrifuged at 4 C. Immediately after the isolation of plasma, hydrogen chloride was added to the sample to a final concentration of 0.1 N. Samples were then diluted into an equal volume of saline. Samples were then loaded onto a Sep-Pak C18 cartridge (Waters, Milford, MA) preequilibrated in 0.1% trifluoroacetic acid (TFA) and 0.9% NaCl. After washing the cartridges with 0.9% NaCl and 5% acetonitrile (CH_3CN)/0.1% TFA, samples were eluted in 60% CH_3CN/0.1% TFA. The eluates were lyophilized; residual materials were redissolved in 1 M AcOH and adsorbed onto a SP-Sephadex C-25 column (H^+-form, Pharmacia, Uppsala, Sweden) preequilibrated in 1 M AcOH. Successive elution in 1 M AcOH, 2 M pyridine, and 2 M pyridine-AcOH (pH 5.0) generated three fractions: SP-I, SP-II, and SP-III. The SP-III fraction was first evaporated and redissolved in 1 M AcOH and then separated by reverse-phase HPLC with C18-cartridge (C18 RP-HPLC) (Symmetry 300, 3.9 × 150 mm, Waters) using a linear gradient from 10 to 60% CH_3CN/0.1% TFA at a flow rate of 1.0 ml/min for 40 min, collecting 500-μl fractions. Ghrelin peptide content in each fraction was determined by ghrelin C-RIA as described above.

Concentration and acyl modification of ghrelin after free fatty acid (FFA) or triacylglycerol ingestion

The standard laboratory chow, CE-2 (CLEA Rodent Diet CE-2, CLEA Japan, Osaka, Japan), contained a caloric content of approximately 50.3% carbohydrate, 25.4% protein, and 4.4% fat. MCFAs, such as *n*-hexanoic, *n*-octanoic, and *n*-lauric acid (Sigma-Aldrich Japan Co. Ltd., Tokyo, Japan), were dissolved in water at 5 mg/ml. To equilibrate the total intake of *n*-palmitic acid to the other MCFAs contained in food, this common long-chain fatty acid (Sigma-Aldrich Japan) was mixed into CE-2 chow at a concentration of 1% (wt/wt). Medium- and long-chain triglycerides (MCTs and LCTs), including glyceryl trihexanoate, trioctanoate, tridecanoate, and tripalmitate (Wako Pure Chemical, Osaka, Japan), were mixed into CE-2 chow at a concentration of 5% (wt/wt). Whole-stomach tissues from mice were collected at the indicated times (0–14 d) after the beginning of treatment. To elucidate the forms of ghrelin peptides modified by different acyl groups, stomach peptides, extracted as described above, were collected using a Sep-Pak Plus C18 cartridge (Waters). The recovery of des-acyl, *n*-hexanoyl, *n*-octanoyl, *n*-decanoyl, *n*-lauryl, and *n*-palmitoyl ghrelin from the Sep-Pak C18 cartridges were over 90%. The extracted peptides were subjected to C18 RP-HPLC (Symmetry 300, 3.9 × 150 mm, Waters) using a linear gradient from 10 to 60% CH_3CN/0.1% TFA at a flow rate of 1.0 ml/min for 40 min and collected in 500-μl fractions. The ghrelin peptide content in each fraction was measured by ghrelin C- and N-RIA as described above. No ghrelin degradation was observed during the extraction.

Concentration and acyl modification of ghrelin after high-fat (HF) diet ingestion

To examine the effect of dietary LCTs on the distribution of stomach acyl-modified or des-acyl ghrelin, we fed mice a HF diet enriched in LCTs, in which nearly 50% of the total calories originated from animal fat. This HF diet, modified from an AIN-76A standard chow, derived approximately 35.4% of the total caloric content from carbohydrates, 16.2% from protein, and 48.4% from fat (24). By caloric content, AIN-76A chow contained 69.2% carbohydrate, 18.4% protein, and 12.4% fat. We fed male C57BL/6J mice the HF diet for 2 wk and then compared the distribution of stomach ghrelin with that seen in control mice fed standard AIN-76A chow. The distribution of stomach ghrelin molecules was

Downloaded from endo.endojournals.org on March 19, 2006

measured using ghrelin C-RIA after HPLC fractionation, as described above.

Northern blot analysis

Total RNAs were extracted from the stomachs of male C57BL/6J mice (12 wk old) by acid guanidium thiocyanate-phenol chloroform extraction (25) using TRIzol Reagent (Invitrogen, Carlsbad, CA). Two micrograms of total RNA were electrophoresed on a 1% agarose gel containing formaldehyde and then transferred to a ζ-probe-blotting membrane (Bio-Rad Laboratories, Hercules, CA). A ^{32}P-labeled rat ghrelin cDNA probe was hybridized to the membranes in hybridization buffer, containing 50% formamide, 5× sodium-chloride sodium-phosphate EDTA buffer, 5× Denhardt's solution, 1% sodium dodecyl sulfate, and 100 μg/ml denatured salmon sperm. After overnight hybridization at 37 C, membranes were washed and exposed to BioMax-MS film (Eastman Kodak, Rochester, NY) for 12 h at −80 C. Ghrelin mRNA levels were quantified using a BAS 2000 bioimaging analyzer (Fujix, Tokyo, Japan).

Purification of n-heptanoyl ghrelin

n-Heptanoyl ghrelin was purified as described for the purification of ghrelin using antirat ghrelin(1–11) IgG immunoaffinity chromatography (22). During purification, ghrelin activity was assayed by measuring the changes in intracellular calcium concentrations using a FLEX station (Molecular Devices) in a cell line stably expressing rat GHS-R (CHO-GHSR62). Ghrelin C-RIA was also used to monitor ghrelin immunoreactivity in isolated samples.

Glyceryl triheptanoate (Fluka Chemie GmbH, Buchs, Switzerland) was mixed with standard laboratory chow at a concentration of 5% (wt/wt). Four days after mice (n = 7) were fed glyceryl triheptanoate-containing food, we collected stomachs (total 1000 mg). The total consumption of glyceryl triheptanoate-containing food was approximately 13.5 g/mouse, equivalent to 675 mg total glyceryl triheptanoate ingested by each mouse. Stomachs were prepared and homogenized as described above. After a 30-min centrifugation at 20,000 rpm, homogenization supernatants were loaded onto a Sep-Pak C18 environmental cartridge (Waters) preequilibrated in 0.1% TFA. After washing in 10% CH_3CN/0.1% TFA, peptide fractions were eluted in 60% CH_3CN/0.1% TFA. The eluate was then evaporated and lyophilized. Residual materials were redissolved in 1 M AcOH and fractionated as described above for plasma samples. After application of the lyophilized SP-III fraction to a Sephadex G-50 fine gel-filtration column (1.9 × 145 cm) (Pharmacia), we collected 5-ml fractions. A portion of each fraction was subjected to the ghrelin calcium-mobilization assay. Half of each active fraction (no. 47–51) was collected using a Sep-Pak C18 light cartridge and lyophilized. Samples were then resuspended in 1.0 ml 100 mM phosphate buffer (pH 7.4) and purified by antirat ghrelin(1–11) IgG immunoaffinity chromatography. Adsorbed substances were eluted in 500 μl 10% CH_3CN/0.1% TFA. The eluate was evaporated and separated by RP-HPLC (Symmetry 300, 3.9 × 150 mm, Waters). *n*-Heptanoyl-modified ghrelin was obtained at a retention time of 18.4 min and subjected to a mass spectrometry to confirm the appropriate molecular weight. The amino acid sequences of purified peptides were analyzed using a protein sequencer (494, Applied Biosystems, Foster City, CA).

Mass spectrometric analysis of n-heptanoyl ghrelin

Matrix-assisted laser desorption/ionization time-of-flight mass spectrometry (MALDI-TOF-MS) was performed using a Voyager DE-Pro spectrometer (Applied Biosystems) (26). Mass spectra were recorded in the reflector mode, with an accelerating voltage of 20 kV. Saturated α-cyano-4-hydroxycinnamic acid in 60% CH_3CN and 0.1% TFA were used as a working matrix solution. Approximately 1 pmol of the final purified sample was mixed with the matrix solution, placed on the sample probe, and dried in the air before analysis. All mass spectra were acquired in positive ion mode, averaged by 100 spectra.

Results

The effect of FFA ingestion for the stomach content of total and n-octanoyl ghrelin measured by ghrelin C- and N-RIA

To examine the effect of daily ingestion of FFAs on the acyl modification of ghrelin, we extracted gastric peptides from mice given *ad libitum* access to water containing *n*-hexanoic acid, *n*-octanoic acid, or *n*-lauric acid or chow containing *n*-palmitic acid. The stomach concentration of *n*-octanoy-modified and total (*n*-octanoylated plus des-acyl) ghrelin forms were measured by ghrelin N- and C-RIA, respectively. The stomach content of *n*-decanoyl, *n*-decanoyl, and *n*-hexanoyl ghrelins in mice fed normal chow was low in comparison to *n*-octanoyl ghrelin (see Fig. 3 and Table 1). The reactivity of N-RIA for *n*-decanoyl-, *n*-decanoyl-, and *n*-hexanoyl-modified ghrelins is low, compared with that seen for *n*-octanoyl ghrelin; thus, the concentration of acyl-modified ghrelin measured by N-RIA primarily reflects *n*-octanoyl ghrelin. During the experimental period (0–14 d), no significant differences between the fatty acid-ingesting and control groups in mouse body weight or total dietary consumption were observed.

After a 14-d administration of *n*-hexanoic acid, *n*-octanoic acid, *n*-lauric acid, or *n*-palmitic acid, we compared the gastric concentrations of *n*-octanoyl and total ghrelin with concentrations seen in control mice fed normal chow and water. The gastric concentrations of *n*-octanoyl ghrelin increased significantly in mice fed *n*-octanoic acid (Fig. 1A). The mean stomach concentrations of *n*-octanoyl ghrelin were 1795 fmol/mg wet weight in control rats fed normal food (n = 8) and 2455 fmol/mg wet weight in mice fed *n*-octanoic acid-containing food (n = 8). No significant changes were observed in the total ghrelin concentrations measured by C-RIA (Fig. 1B). Therefore, the ratio of *n*-octanoyl ghrelin/total ghrelin increased significantly in mice fed *n*-octanoic acid (Fig. 1C). No significant changes in the stomach contents of total

TABLE 1. Concentrations of des-acyl and acyl-modified ghrelins in the stomachs of mice after ingestion of medium-chain (C6:0-C10:0) triglycerides

	des-acyl Ghrelin	C6:0-ghrelin	C8:0-ghrelin	C10:0-ghrelin	Total ghrelin
Control	301.7 ± 19.0	28.6 ± 3.5	531.1 ± 27.3	30.8 ± 5.5	1146.6 ± 75.4
C6:0-MCT	253.7 ± 4.4	237.8 ± 34.8[a]	360.8 ± 33.3[a]	25.8 ± 6.0	1075.4 ± 46.0
C8:0-MCT	227.2 ± 34.9[b]	12.3 ± 4.5	788.8 ± 82.6[a]	8.8 ± 5.7[a]	1145.1 ± 95.8
C10:0-MCT	207.5 ± 27.0[c]	24.6 ± 4.4	516.9 ± 42.3	108.4 ± 12.0[a]	958.7 ± 84.2[b]

Male C57BL/6J mice were fed chow mixed with 5% (wt/wt) glyceryl trihexanoate (C6:0-MCT), glyceryl trioctanoate (C8:0-MCT), or glyceryl tridecanoate (C10:0-MCT) for 14 d. The concentrations of des-acyl ghrelin, *n*-hexanoyl ghrelin (C6:0-ghrelin), *n*-octanoyl ghrelin (C8:0-ghrelin), *n*-decanoyl ghrelin (C10:0-ghrelin), and total ghrelin in stomach samples (from 0.2 mg wet weight) were measured by ghrelin C-RIA after HPLC fractionation. Data represent mean ± SD of six samples.

[a] $P < 0.001$.

[b] $P < 0.05$.

[c] $P < 0.01$ *vs.* control.

Downloaded from endo.endojournals.org on March 19, 2006

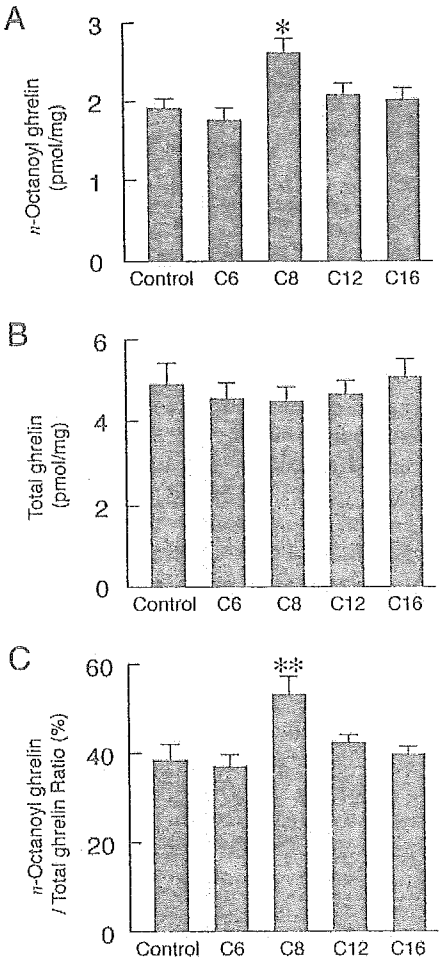

FIG. 1. Ghrelin concentrations in the stomachs of normal control animals (control) fed standard chow and water and mice fed *n*-hexanoic acid (C6), *n*-octanoic acid (C8), *n*-lauric acid (C12), or *n*-palmitic acid (C16). A, *n*-Octanoyl ghrelin concentrations measured by ghrelin N-RIA (n = 8). Because N-RIA is highly specific for *n*-octanoyl ghrelin, exhibiting low cross-reactivity to other acylated forms of ghrelin such as *n*-hexanoyl, *n*-lauryl, or *n*-palmitoyl ghrelin, the concentration of acyl-modified ghrelin measured by N-RIA primarily reflects *n*-octanoyl ghrelin. B, Total ghrelin concentrations measured by ghrelin C-RIA (n = 8), including both acylated and des-acyl ghrelin. The C-RIA equally recognizes all des-acyl and acylated forms of ghrelin containing an intact C-terminal sequence. C, Ratios of acyl-modified to total ghrelin. Data represent mean ± SD of ghrelin concentrations in stomach extracts (from 1 mg wet weight). Statistical significance is indicated by *asterisks*. *, $P < 0.01$; **, $P < 0.001$ *vs.* control.

ghrelin measured by C-RIA could be observed after treatment with *n*-hexanoic, *n*-decanoic, or *n*-palmitic acids. After this treatment, no significant differences were detected in the stomach content of *n*-octanoyl ghrelin. Thus, the exogenously supplied *n*-octanoic acid specifically increased gastric concentrations of *n*-octanoyl ghrelin without altering the total quantities of ghrelin peptide.

The effect of triacylglycerol ingestion for the stomach content of total and n-octanoyl ghrelin measured by ghrelin C- and N-RIAs

Orally ingested triacylglycerols are intraluminally hydrolyzed and absorbed through the gastrointestinal mucosa as FFAs or monoglycerides. Thus, ingested triacylglycerols may serve as a source of FFAs (27). To examine whether ingested triacylglycerols are used for acyl modification of ghrelin, mice were fed chow mixed with 5% (wt/wt) glyceryl trihexanoate, trioctanoate, tridecanoate, and tripalmitate. All mice were given *ad libitum* access to experimental food and water. After 2 wk, we measured the content of *n*-octanoyl and total ghrelin in extracted gastric peptides by N- and C-RIAs. Glyceryl trioctanoate ingestion increased stomach concentrations of *n*-octanoyl ghrelin (Fig. 2A). In contrast, glyceryl trihexanoate ingestion decreased the stomach contents of *n*-octanoyl ghrelin identified by ghrelin N-RIA. Mice fed glyceryl trihexanoate, however, exhibited increased concentrations of *n*-hexanoyl ghrelin (Fig. 3 and Table 1). Ingestion of glyceryl tridecanoate and glyceryl tripalmitate had no effect on the production of *n*-octanoylated ghrelin (Fig. 2A)

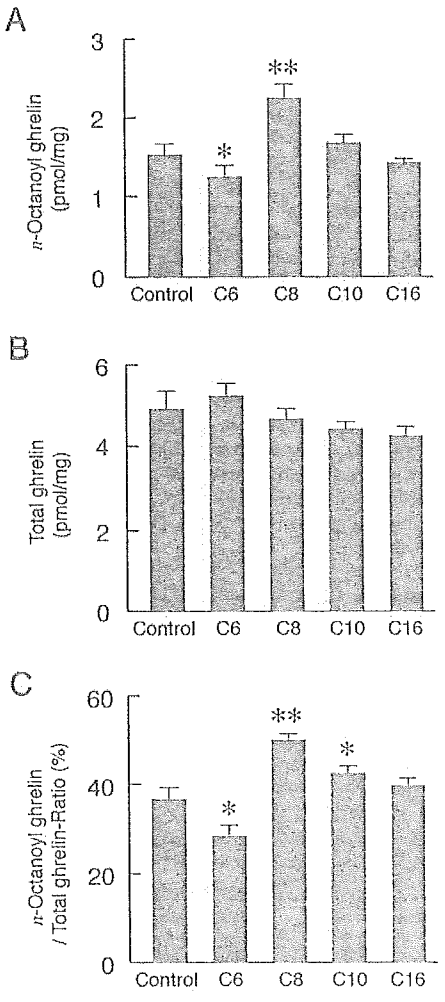

FIG. 2. Ghrelin concentration in the stomachs of mice fed standard laboratory chow (control) (n = 8) and mice fed chow containing glyceryl trihexanoate (C6), trioctanoate (C8), tridecanoate (C10), or tripalmitate (C16). A, *n*-Octanoyl ghrelin concentrations were measured by ghrelin N-RIA. B, Total ghrelin concentrations were measured by ghrelin C-RIA. Data represent the mean ± SD of ghrelin concentrations in stomach extracts (from 1 mg wet weight) (n = 5). C, The ratio of *n*-octanoyl to total ghrelin. Data represent mean ± SD of calculated ratios (n = 5). Statistical significance is indicated by *asterisks*. *, $P < 0.05$; **, $P < 0.01$ *vs.* control.

Downloaded from endo.endojournals.org on March 19, 2006

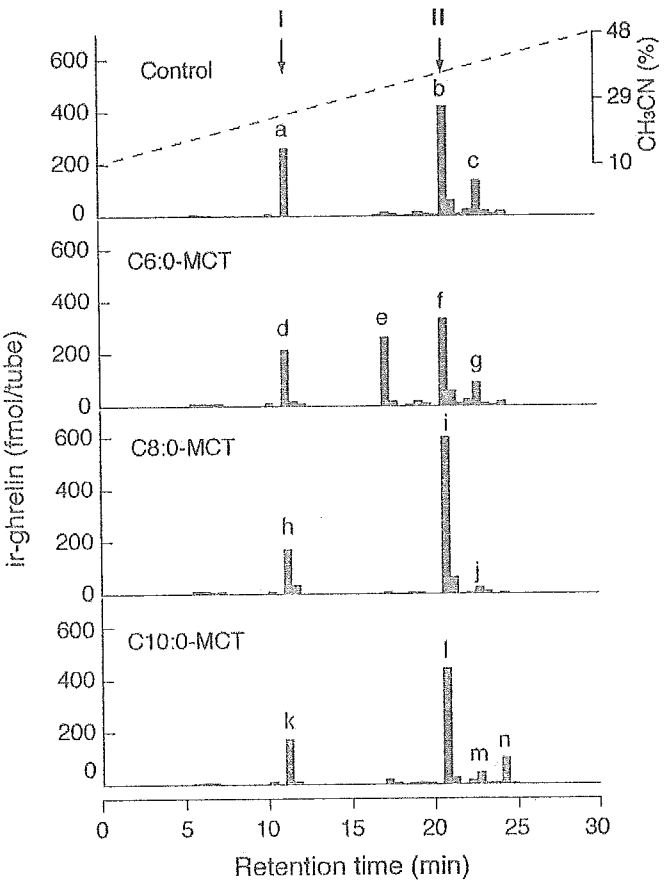

FIG. 3. The molecular forms of ghrelin peptides isolated from the stomachs of mice fed standard laboratory chow (control) or chow containing glyceryl trihexanoate (C6:0-MCT), glyceryl trioctanoate (C8:0-MCT), or glyceryl tridecanoate (C10:0-MCT). Ghrelin immunoreactivity in peptide extracts from mouse stomachs, fractionated by HPLC, was quantitated by C-RIA. Assay tubes contained equivalent quantities of peptide extract derived from 0.2 mg of stomach tissue. *Black bars* represent immunoreactive ghrelin (ir-ghrelin) concentrations determined by ghrelin C-RIA. *Arrows* indicate the elution positions of des-acyl ghrelin (I) and *n*-octanoyl ghrelin (II). Based on the retention times of synthetic ghrelin forms, peaks a, d, h, and k correspond to des-acyl ghrelin, whereas peaks b, f, i, and l correspond to *n*-octanoyl ghrelin. Peaks c, g, j, and m correspond to *n*-decanoyl (C10:1) ghrelin. Peak n corresponds to *n*-decanoyl (C10:0) ghrelin.

or the total stomach concentrations of ghrelin (des-acyl and acyl-modified ghrelins) in five independent groups of mice (Fig. 2B). Therefore, the molar ratios of *n*-octanoyl ghrelin/total ghrelin decreased in glyceryl trihexanoate-treated mice and increased in glyceryl tridecanoate-treated mice (Fig. 2C). Throughout the experimental period (0–2 wk), no significant differences in body weight or total food consumption could be observed between triacylglycerol-fed and control groups.

Molecular forms of ghrelin peptide after triacylglycerol ingestion

To clarify the molecular forms of ghrelin peptide present after triacylglycerol ingestion, we measured ghrelin immunoreactivity by C-RIA in fractions of stomach extracts isolated by HPLC to reveal the ghrelin molecular forms (Fig. 3) present in mice fed glyceryl trihexanoate, trioctanoate, and tridecanoate. Based on the observed retention times of synthetic des-acyl or acyl-modified ghrelin peptides, 11.2 min for des-acyl ghrelin, 13.8 min for *n*-butyryl ghrelin, 17.2 min for *n*-hexanoyl ghrelin, 20.2 min for *n*-octanoyl ghrelin, 22.6 min for *n*-decanoyl ghrelin, 24.2 min for *n*-decanoyl, 27.6 min for *n*-lauryl ghrelin, and 34.6 min for *n*-palmitoyl ghrelin, peaks a, d, h, and k corresponded to a des-acyl ghrelin lacking any fatty acid modification. Peaks b, f, i, and l corresponded to a *n*-octanoyl ghrelin, the form modified at Ser^3 by *n*-octanoic (C8:0) acid. Peaks c, g, j, and m corresponded to a *n*-decanoyl ghrelin form bearing an *n*-decanoic (C10:1) acid modification.

Ingestion of glyceryl trioctanoate stimulated the production of *n*-octanoyl ghrelin (peak i in Fig. 3). The molar ratio of *n*-octanoyl/total ghrelin reached greater than 60% in treated mice (Table 1). This high *n*-octanoyl ghrelin ratio was not observed in mice fed normal food and water (Table 1). Because the stomach content of *n*-octanoyl ghrelin also increased after *n*-octanoic acid ingestion, both glyceryl trioctanoate and *n*-octanoic acid can increase the stomach concentrations of *n*-octanoyl ghrelin.

n-hexanoyl ghrelin could be detected only at very low levels in stomach of mice fed normal chow. When fed glyceryl trihexanoate, however, the stomach concentrations of *n*-hexanoyl ghrelin, bearing the *n*-hexanoic (C6:0) acid modification, increased drastically (peak e). We also observed significant decreases in *n*-octanoyl ghrelin concentrations in these mice (peak f in Fig. 3 and Table 1) in comparison with levels observed in control mice (peak b in Fig. 3 and Table 1). The content of *n*-hexanoyl ghrelin also increased after ingestion of *n*-hexanoic acid (data not shown).

Moreover, after ingestion of glyceryl tridecanoate, the stomach concentration of the *n*-decanoyl ghrelin form modified by *n*-decanoic (C10:0) acid increased (peak n).

Ghrelin peaks eluting at the same retention times as synthetic *n*-butyryl (C4:0), *n*-lauryl (C12:0), and *n*-palmitoyl (C16:0) ghrelin could not be observed in the stomach extracts of mice given glyceryl tributyrate, trilaurate, or tripalmitate (data not shown), indicating that neither glyceryl tributyrate nor tripalmitate could be transferred to ghrelin in mice.

To examine the influence of a high-fat intake on the distribution of des-acyl and acyl-modified ghrelins in mouse stomach, we fed mice a HF diet with 48.4% of the total calories from animal fat containing a high proportion of LCTs. We compared the distribution of stomach ghrelin in mice ingesting the HF diet with control mice fed an AIN-76A control diet (deriving 12.4% of the total calories from fat). We observed a faint, but significant, decrease in both the amount and proportion of des-acyl ghrelin in the stomach after a 2-wk administration of the HF diet (Table 2). We also observed a significant increase in the proportion of total ghrelin that bore the *n*-octanoyl modification (C8:0) in the HF diet group in comparison with the control animals. Whereas the total amount of stomach *n*-decanoyl (C10:0) ghrelin also increased in the HF diet group, we observed a faint decrease in the proportion of total ghrelin that was *n*-decanoylated (C10:1) in the HF diet group. Whereas the total amount of stomach ghrelin decreased slightly in mice fed a HF diet, there was no significant difference between the HF diet and control groups. These changes in the distribution of stomach ghrelins after administering the HF diet were small in com-

Downloaded from endo.endojournals.org on March 19, 2006

TABLE 2. The effect of HF diet on the distribution of stomach ghrelins

Diet	AIN-76A diet	HF diet
Total ghrelin	1058 ± 108	992 ± 122
des-acyl Ghrelin	275.2 ± 39.6 (26.0 ± 2.4)	229.3 ± 46.1[a] (23.0 ± 2.8)[a]
n-Hexanoyl ghrelin	32.8 ± 5.2 (3.1 ± 0.3)	29.4 ± 4.9 (3.0 ± 0.4)
n-Octanoyl ghrelin	452.0 ± 45.2 (42.8 ± 2.0)	464.3 ± 43.7 (48.0 ± 2.4)[b]
n-Decenoyl ghrelin	187.2 ± 17.1 (17.8 ± 1.1)	138.2 ± 19.7[a] (13.9 ± 1.1)[c]
n-Decanoyl ghrelin	33.9 ± 5.1 (3.2 ± 0.3)	38.0 ± 6.7 (3.8 ± 0.6)[a]

The content of each ghrelin molecule was measured by ghrelin C-RIA after HPLC fractionation. Data represent mean ± SD of the amount (fmol/0.2 mg) of each ghrelin molecule (n = 8). Data in *parentheses* represent the proportion (percentage) of each ghrelin molecule for total ghrelin.
[a] $P < 0.05$.
[b] $P < 0.01$.
[c] $P < 0.001$ *vs.* control (AIN-76A diet group).

parison with those observed after treatment with MCFAs or MCTs.

Time course of n-octanoyl ghrelin production after glyceryl trioctanoate ingestion

To examine time-dependent changes in *n*-octanoyl ghrelin production after ingestion of glyceryl trioctanoate, we fed mice glyceryl trioctanoate-containing chow (5%, wt/wt) after a 12-h fasting period. We then measured the stomach concentrations of *n*-octanoyl and total ghrelins at the indicated times. *n*-octanoyl ghrelin production (Fig. 4) increased significantly in the stomach 3 h after the ingestion of glyceryl trioctanoate. When continuously given glyceryl trioctanoate, the stomach concentrations of *n*-octanoyl ghrelin gradually increased, peaking 24 h after the beginning of administration. The stomach concentrations of *n*-octanoyl ghrelin measured 14 d after continuous feeding of the glyceryl trioctanoate-mixed chow remained significantly higher than those of mice fed normal chow (Fig. 4A). Under these conditions, however, no significant changes in the stomach content of total ghrelin, measured by C-RIA, could be observed (Fig. 4B).

Ghrelin mRNA expression after glyceryl trioctanoate ingestion

To examine whether the ingestion of MCTs affects ghrelin mRNA expression, we quantitated ghrelin RNA in mouse stomach by Northern blot analysis after 4 d of glyceryl trioctanoate ingestion (Fig. 5). The expression levels of gastric ghrelin mRNA did not change after the ingestion of glyceryl trioctanoate. Because the ingestion of glyceryl trioctanoate increased the stomach content of *n*-octanoyl ghrelin without changing the total ghrelin concentration, we propose that ingestion of glyceryl trioctanoate stimulates the octanoyl modification of ghrelin only.

Molecular forms of ghrelin peptides after glyceryl triheptanoate ingestion

To examine the direct use of ingested FFAs for acyl modification of ghrelin, mice were fed MCTs that are not present in food sources nor naturally synthesized in mammals. We selected synthetic glyceryl triheptanoate as an unnatural FFA source because *n*-heptanoic acid (C7:0), a hydrolyzed from of glyceryl triheptanoate, does not naturally occur in mammals. Moreover, *n*-heptanoyl ghrelin can be easily separated from natural ghrelin by HPLC. We examined ghrelin content in stomach extracts from mice fed glyceryl triheptanoate by examining ghrelin immunoreactivity by C-RIA in HPLC fractions. The retention times of the peaks a and c corresponded to des-acyl ghrelin and *n*-octanoyl ghrelin, respectively (Fig. 6). Peak b immunoreactivity was observed only in mice fed glyceryl triheptanoate. This peak was not observed in mice fed any of the other FFAs or triglycerides examined, including *n*-hexanoic acid, *n*-octanoic acid, *n*-lau-

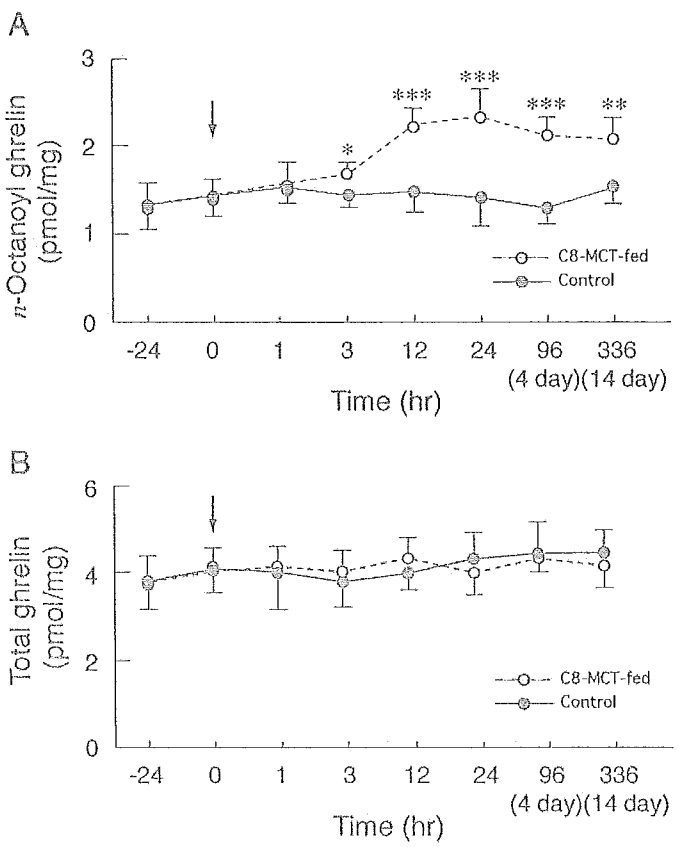

FIG. 4. Time-dependent changes in stomach concentrations of ghrelin in mice fed glycerol trioctanoate. A, *n*-Octanoyl ghrelin content was measured by ghrelin N-RIA. B, Total ghrelin content was measured by ghrelin C-RIA. After 12 h of fasting, mice were given glyceryl trioctanoate (5% wt/wt)-containing food beginning at the time (0 h) indicated by the *arrow*. Stomach samples were isolated from control mice fed standard laboratory chow (*closed circles*) and mice fed glyceryl trioctanoate (C8-MCT; *open circles*) at the indicated times. Each point represents mean ± SD (n = 8). Statistical significance is indicated by *asterisks*. *, $P < 0.05$; **, $P < 0.01$; ***, $P < 0.001$ *vs.* control.

Downloaded from endo.endojournals.org on March 19, 2006

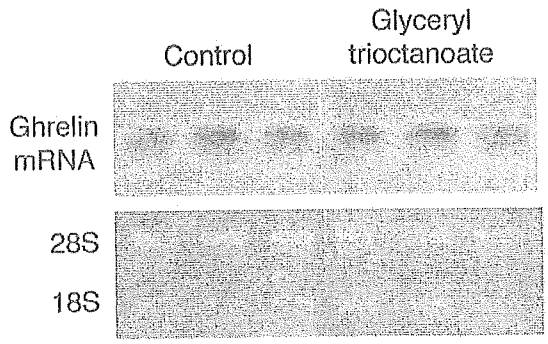

FIG. 5. Northern blot analysis examining stomach ghrelin mRNA expression after ingestion of glyceryl trioctanoate-containing food. Each lane contained 2 μg of total RNA. The *lower panel* indicates the intensity of 28S and 18S rRNAs internal controls.

ric acid, *n*-palmitic acid, and the corresponding triglyceride forms. The estimated retention time of peak b was between that of *n*-hexanoyl and *n*-octanoyl ghrelin, consistent with *n*-heptanoyl ghrelin.

Purification of n-heptanoyl ghrelin

To confirm the use of the ingested glyceryl triheptanoate for *n*-heptanoyl ghrelin modification, we purified acyl-modified ghrelins from the stomachs of mice fed glyceryl triheptanoate-containing food for 4 d. This purification of ghrelin peptides from the stomachs of treated mice identified peak

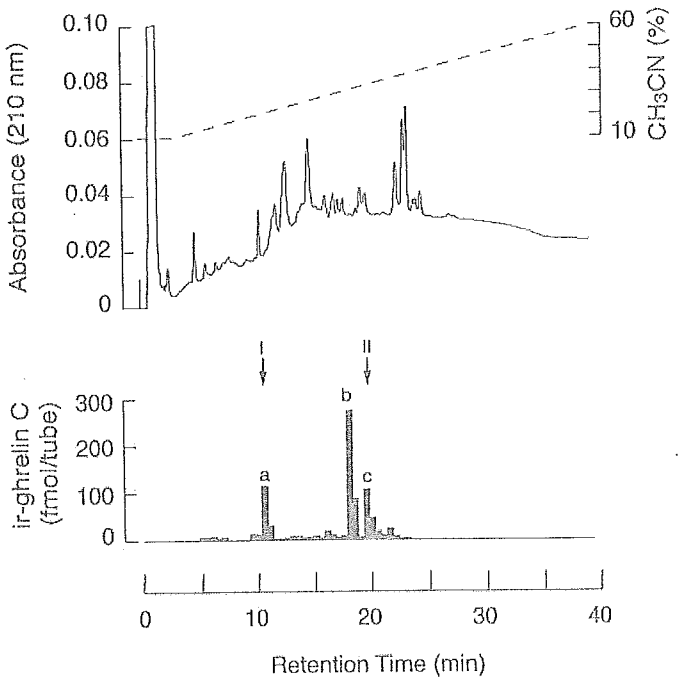

FIG. 6. The HPLC profile of peptides extracted from the stomachs of mice fed glyceryl triheptanoate. Stomach extracts of glyceryl triheptanoate-treated mice were fractionated by HPLC (*upper panel*). The concentration of ghrelin in each fraction (equivalent to 0.2 mg stomach tissue) was monitored by C-RIA (*lower panel*). Ghrelin immunoreactivity (ir-ghrelin),represented by *solid bars*, was separated into three major peaks (peaks a, b, and c) by C-RIA. Peak b was observed only after the ingestion of glyceryl triheptanoate. *Arrows* indicate the elution positions of des-acyl ghrelin (I) and *n*-octanoyl (II) ghrelin.

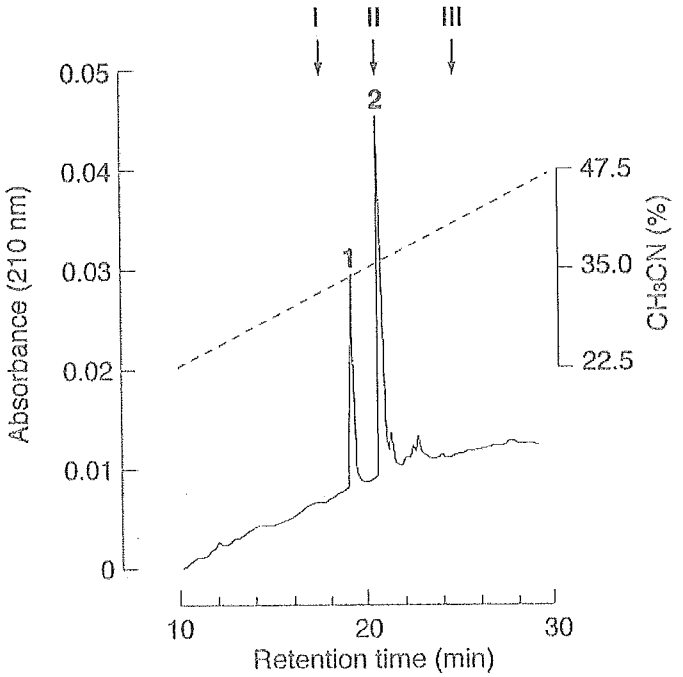

FIG. 7. Purification of *n*-heptanoyl ghrelin. Ghrelin peptides were purified from the stomachs of mice fed glyceryl triheptanoate. Samples eluted from an antirat ghrelin immunoaffinity column were subjected to HPLC. Peak 1 was observed only in samples from glyceryl triheptanoate-treated mice. Based on the retention times of control samples in HPLC and MALDI-TOF-MS analysis, peak 2 corresponded to *n*-octanoyl ghrelin. *Arrows* indicated the elution positions of *n*-hexanoyl (I), *n*-octanoyl (II), and *n*-decanoyl (III) ghrelin.

2 (Fig. 7) as *n*-octanoyl ghrelin from its HPLC retention time. The extra peak eluting at a retention time of 18.4 min (peak 1 in Fig. 7), observed only after ingestion of glyceryl triheptanoate, eluted at a retention time between that of *n*-hexanoyl- and *n*-octanoyl ghrelin. We purified this peak 1 peptide and subjected it to amino acid sequence analysis and mass spectrometry.

The purified HPLC peak 1 peptide (Fig. 7) contained 28 amino acids with an identical amino acid sequence to that of mouse ghrelin. The average m/z value of the peak 1 peptide measured by MALDI-TOF-MS was 3301.9 (Fig. 8A). The estimated molecular weight of this peptide, calculated from this MALDI-TOF-MS m/z value, was 3300.9. Modification of ghrelin at Ser^3 with an *n*-heptanoyl group would produce a theoretical molecular weight of approximately 3300.86 (Fig. 8B), an almost identical molecular weight as that measured by MALDI-TOF-MS. Thus, we concluded that the purified peak 1 peptide was *n*-heptanoyl ghrelin. No additional peaks were observed in the final purification, indicating that, after hydrolysis from the ingested glyceryl triheptanoate, the *n*-heptanoyl group could be directly transferred to Ser^3 of ghrelin.

Molecular forms of circulating ghrelin peptides after glyceryl triheptanoate ingestion

To examine whether *n*-heptanoyl ghrelin synthesized after glyceryl triheptanoate ingestion is secreted into the circulation, we determined the molecular forms of acyl-modified

Downloaded from endo.endojournals.org on March 19, 2006

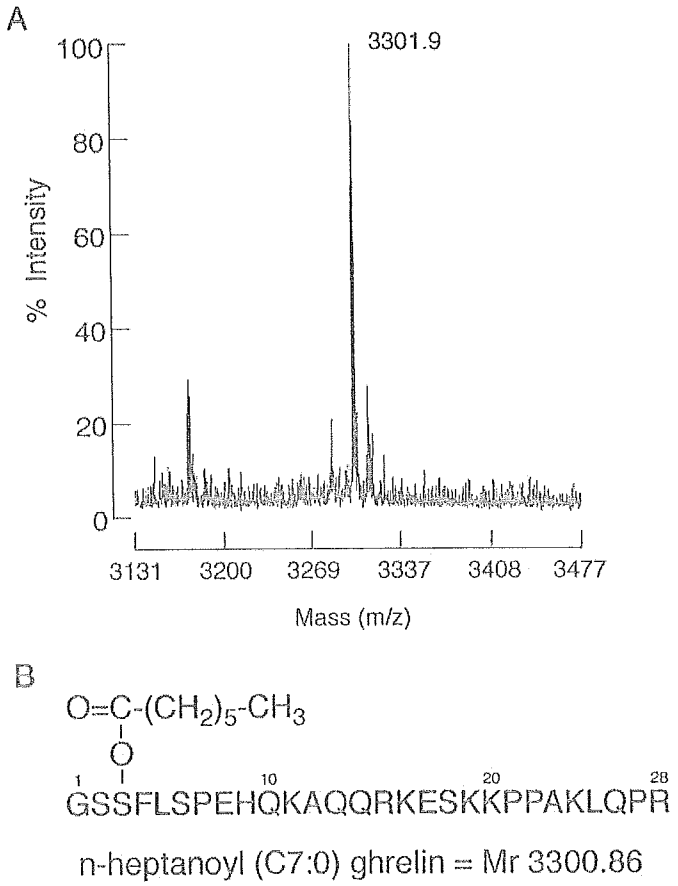

FIG. 8. A, MALD-TOF-MS of the purified ghrelin-like peptide in Fig. 7, peak a. The mass ranges from 3131.0 to 3477.0 (m/z). From the average of 100 mass spectra acquired in positive ion mode (average $[M+H]^+$: 3301.9), the molecular weight of the peak a peptide was calculated to be 3300.9. B, The structure of *n*-heptanoyl (C7:0) ghrelin provides a calculated molecular weight for *n*-heptanoyl ghrelin of 3300.86.

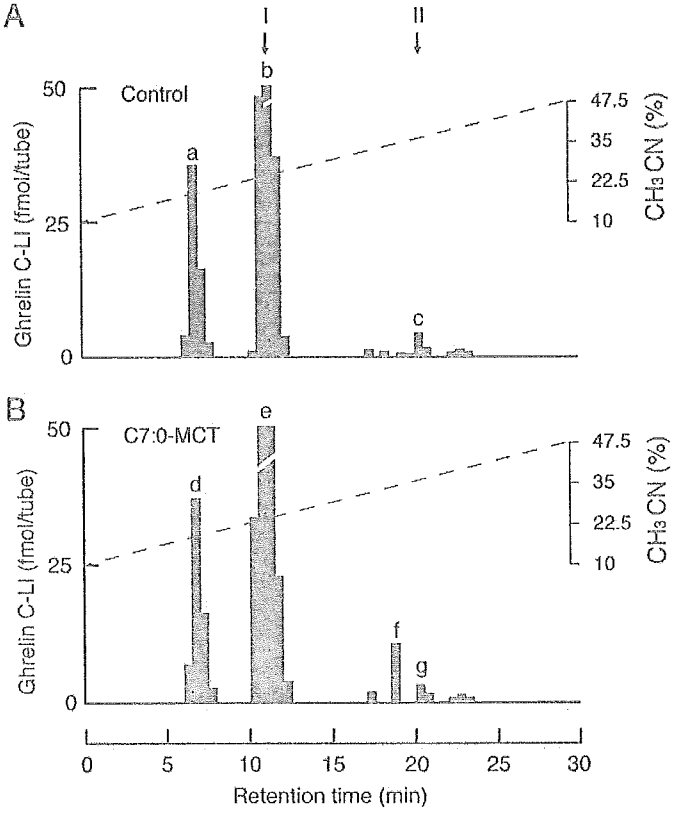

FIG. 9. The molecular forms of plasma ghrelin peptides isolated from mice fed glyceryl triheptanoate-containing chow. Plasma samples from mice fed standard chow (A) or glyceryl triheptanoate-containing food (B) were fractionated by HPLC. Ghrelin immunoreactivity was then measured by C-RIA. *Arrows* indicate the elution positions of des-acyl ghrelin (I) and *n*-octanoyl ghrelin (II). Plasma ghrelin immunoreactivity is represented by *solid bars*. Based on the retention times of each peak, peaks b and e correspond to des-octanoyl ghrelin, whereas peaks c and g correspond to *n*-octanoyl ghrelin. Peak f exhibited a similar elution profile as that of *n*-heptanoyl ghrelin isolated from the stomachs of mice given glyceryl triheptanoate.

ghrelin found in the plasma of mice fed glyceryl triheptanoate-containing food for 4 d (Fig. 9, A and B). Plasma samples, fractionated by RP-HPLC, were assessed for ghrelin immunoreactivity by C-RIA. Plasma ghrelin immunoreactivity in control mice was separated into two major peaks (peaks a and b in Fig. 9A) and a minor peak (peak c in Fig. 9A). Plasma ghrelin immunoreactivity in glyceryl triheptanoate-treated mice was separated into two major peaks (peaks d and e in Fig. 9B) and two minor peaks (peaks f and g in Fig. 9B). Based on the elution profiles, peaks b and e corresponded to *des*-acyl ghrelin, whereas peaks c and g corresponded to *n*-octanoyl ghrelin. Although peaks a and d are thought to be a C-terminal fragment of the ghrelin peptide resulting from protease digestion, the exact molecular form of this peptide has not yet been determined.

Peak f, which eluted at 18.0–18.5 min, was observed only in samples from glyceryl triheptanoate-treated mice. This analysis revealed the existence of a plasma ghrelin molecule with the same retention time as that of *n*-heptanoyl ghrelin purified from the stomachs of glyceryl triheptanoate-fed mice (peak f in Fig. 9B). These results indicate that despite the fact that *n*-heptanoyl ghrelin is an unnatural form of ghrelin synthesized *in vivo* after glyceryl triheptanoate ingestion, it can be released into the circulation.

Activity of n-heptanoyl ghrelin

Using the ghrelin calcium-mobilization assay, we examined GHS-R-stimulating activity of *n*-heptanoyl ghrelin purified from glyceryl triheptanoate-ingested mouse stomach. *n*-heptanoyl ghrelin induced intracellular-free calcium concentration $[Ca^{2+}]_i$ increases in GHS-R-expressing cells. The time course of these $[Ca^{2+}]_i$ changes was similar to those induced by *n*-octanoyl ghrelin (Fig. 10). Whereas the agonistic activity of *n*-heptanoyl ghrelin for GHS-R, calculated from the area under the curve (AUC) of the response curve, was approximately 60% that of *n*-octanoyl ghrelin, it was 3 times higher than that of *n*-hexanoyl ghrelin (Fig. 10). Thus, *n*-heptanoyl ghrelin possesses GHS-R-stimulating activity.

Discussion

We demonstrate here that ingested MCFAs and MCTs increase the stomach concentrations of acylated ghrelin without increasing either total peptide (measured by ghrelin C-

Downloaded from endo.endojournals.org on March 19, 2006

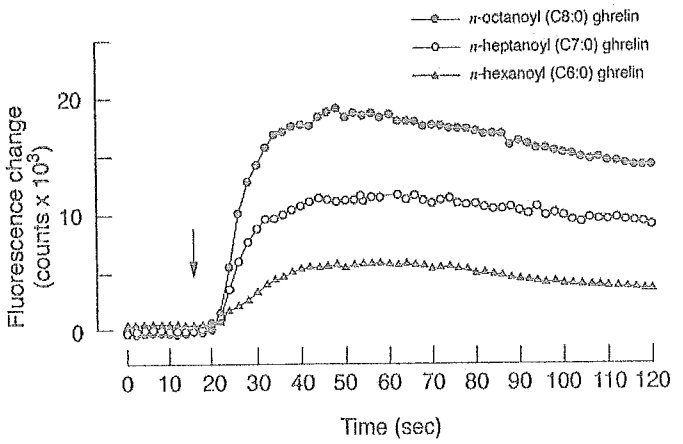

FIG. 10. Time course of fluorescence changes as a measure of $[Ca^{2+}]_i$ changes induced by *n*-octanoyl ghrelin (*closed circle*), *n*-heptanoyl ghrelin (*open circle*), and *n*-hexanoyl ghrelin (*closed triangle*) in GHS-R-expressing cells. Peptides (1×10^{-8} M) were added at the time indicated by the *arrow*.

RIA) or mRNA expression of ghrelin. These exogenous MCFAs and MCTs are directly used for ghrelin acyl modification. Ingestion of synthetic glyceryltriheptanoate or *n*-heptanoic acid produces an *n*-heptanoyl ghrelin that does not occur naturally, supporting the hypothesis of the direct use of MCFAs and MCTs as a fatty acid source for ghrelin acyl modification.

A putative ghrelin-specific acyl-modifying enzyme, ghrelin ser *O*-acyltransferase, may catalyze the acyl modification of *n*-hexanoyl, *n*-heptanoyl, *n*-octanoyl, and *n*-decanoyl ghrelins. Because we could not detect *n*-butyryl or *n*-palmitoyl ghrelin after ingestion of glyceryl tripalmitate, LCTs, or the short-chain triacylglyceride glyceryl tributyrate, the putative acyl-modifying enzyme may prefer MCTs (composed of C6:0-C10:0 FFAs) over either short-chain triacylglycerides or LCTs. Detailed *in vitro* studies will be required to examine the substrate specificity of this putative enzyme.

Ingested triacylglycerides are not the only source of FFAs used in mammals. In a dynamic triglyceride/fatty acid cycle (28), after storage in cells, triacylglycerides can be hydrolyzed, released into the circulation, and transferred to target tissues. Circulating protein-conjugated triglycerides can also be hydrolyzed to FFAs and again transferred to target cells. After conversion to the respective acyl-CoAs by acyl-CoA synthetase, reabsorbed FFAs within target tissues are used to produce ATP or are converted back into triglycerides (29, 30). *n*-octanoyl-CoA is a substrate for carnitine octanoyltransferase, a ubiquitously expressed enzyme abundant in gastrointestinal tissues, such as the stomach (31–34). Thus, *n*-octanoic acid and its derivatives are likely synthesized and stored in cells of this lineage. Thus, even in normal feeding conditions, *n*-octanoyl derivatives produced in normal lipid metabolism may serve as substrates for acyl modification of ghrelin.

Lee *et al.* (24) previously demonstrated that HF diets significantly lowered the rate of stomach ghrelin synthesis, as measured by ghrelin mRNA expression, and secretion, as determined by total ghrelin plasma levels. In contrast, a low-protein, high-carbohydrate diet increased the rate of stomach ghrelin synthesis and secretion (24). Although there were no significant changes in the amount of stomach total ghrelin in each of these feeding conditions, changes in the rate of ghrelin production and secretion may exert some influence on the proportion of acyl-modified ghrelin in the mouse stomach. In our HF diet experiment, we observed a faint, but significant, increase in the proportion of stomach *n*-octanoyl ghrelin in conjunction with a decrease in the levels of stomach *des*-acyl ghrelin. The effect of glyceryl trioctanoate (C8:0-MCT) on the amount and proportions of stomach *n*-octanoyl ghrelin, however, was far greater than that of the HF diet. These findings suggest that ghrelin acyl-modification after ingestion of MCT uses a slightly different mechanistic pathway than that used after administration of a HF diet.

In addition to new insights into the mechanism governing acyl modification of ghrelin, our experiments have also shed light on the role of MCTs in ghrelin synthesis. It is interesting to reexamine the physiological effects of MCT, a naturally occurring component of coconut oil, butter, and other palm kernel oils (27, 35) that is also present in milk from rodents (36) and humans (37, 38), on ghrelin synthesis, modification, and activity. Through the acyl modification of Ser^3, these orally ingested MCTs may modify the ghrelin biological activity.

Whereas both further *in vivo* and *in vitro* studies will be required to elucidate the mechanism of ghrelin acyl modification, our study provides a number of important clues enhancing our understanding of this process. In addition, modification of ghrelin activity through administration of exogenous FFAs may be a potential therapeutic modality for the clinical manipulation of energy metabolism.

Acknowledgments

We thank K. Shirouzu and Y. Yamashita for their technical assistance.

Received June 1, 2004. Accepted January 14, 2005.

Address all correspondence and requests for reprints to: Masayasu Kojima, M.D., Ph.D., Molecular Genetics, Institute of Life Science, Kurume University, Kurume-city, Fukuoka 839-0861, Japan. E-mail-1: mkojima@lsi.kurume-u.ac.jp; or nishi@lsi.kurume-u.ac.jp.

This work was supported by the Program for Promotion of Basic Research Activities for Innovative Biosciences; a Grant-in-Aid for Scientific Research (B) from the Ministry of Education, Culture, Sports, Science, and Technology of Japan; the Uehara Foundation; the Yamanouchi Foundation for Research on Metabolic Disorders; the Takeda Science Foundation; the Brain Science Foundation; the Naito Foundation; the Japan Foundation for Applied Enzymology; a Grant-in-Aid from the Tokyo Biochemical Research; and the Mitsubishi Foundation (to M.K.), MEXT Open Research Project (2004). This work was also supported by a Grant-in-Aid for the Promotion of Fundamental Studies in Health Science from the Organization for Pharmaceutical Safety and Research of Japan (to K.K.).

References

1. Kojima M, Hosoda H, Date Y, Nakazato M, Matsuo H, Kangawa K 1999 Ghrelin is a growth-hormone-releasing acylated peptide from stomach. Nature 402:656–660
2. Hosoda H, Kojima M, Matsuo H, Kangawa K 2000 Ghrelin and des-acyl ghrelin: two major forms of rat ghrelin peptide in gastrointestinal tissue. Biochem Biophys Res Commun 279:909–913
3. Date Y, Kojima M, Hosoda H, Sawaguchi A, Mondal MS, Suganuma T, Matsukura S, Kangawa K, Nakazato M 2000 Ghrelin, a novel growth hormone-releasing acylated peptide, is synthesized in a distinct endocrine cell

Downloaded from endo.endojournals.org on March 19, 2006

type in the gastrointestinal tracts of rats and humans. Endocrinology 141: 4255–4261
4. Date Y, Nakazato M, Hashiguchi S, Dezaki K, Mondal MS, Hosoda H, Kojima M, Kangawa K, Arima T, Matsuo H, Yada T, Matsukura S 2002 Ghrelin is present in pancreatic α-cells of humans and rats and stimulates insulin secretion. Diabetes 51:124–129
5. Mori K, Yoshimoto A, Takaya K, Hosoda K, Ariyasu H, Yahata K, Mukoyama M, Sugawara A, Hosoda H, Kojima M, Kangawa K, Nakao K 2000 Kidney produces a novel acylated peptide, ghrelin. FEBS Lett 486:213–216
6. Galas L, Chartrel N, Kojima M, Kangawa K, Vaudry H 2002 Immunohistochemical localization and biochemical characterization of ghrelin in the brain and stomach of the frog Rana esculenta. J Comp Neurol 450:34–44
7. Gnanapavan S, Kola B, Bustin SA, Morris DG, McGee P, Fairclough P, Bhattacharya S, Carpenter R, Grossman AB, Korbonits M 2002 The tissue distribution of the mRNA of ghrelin and subtypes of its receptor, GHS-R, in humans. J Clin Endocrinol Metab 87:2988
8. Arvat E, Di Vito L, Broglio F, Papotti M, Muccioli G, Dieguez C, Casanueva FF, Deghenghi R, Camanni F, Ghigo E 2000 Preliminary evidence that ghrelin, the natural GH secretagogue (GHS)-receptor ligand, strongly stimulates GH secretion in humans. J Endocrinol Invest 23:493–495
9. Peino R, Baldelli R, Rodriguez-Garcia J, Rodriguez-Segade S, Kojima M, Kangawa K, Arvat E, Ghigo E, Dieguez C, Casanueva FF 2000 Ghrelin-induced growth hormone secretion in humans. Eur J Endocrinol 143:R11–R14
10. Takaya K, Ariyasu H, Kanamoto N, Iwakura H, Yoshimoto A, Harada M, Mori K, Komatsu Y, Usui T, Shimatsu A, Ogawa Y, Hosoda K, Akamizu T, Kojima M, Kangawa K, Nakao K 2000 Ghrelin strongly stimulates growth hormone release in humans. J Clin Endocrinol Metab 85:4908–4911
11. Nakazato M, Murakami N, Date Y, Kojima M, Matsuo H, Kangawa K, Matsukura S 2001 A role for ghrelin in the central regulation of feeding. Nature 409:194–198
12. Shintani M, Ogawa Y, Ebihara K, Aizawa-Abe M, Miyanaga F, Takaya K, Hayashi T, Inoue G, Hosoda K, Kojima M, Kangawa K, Nakao K 2001 Ghrelin, an endogenous growth hormone secretagogue, is a novel orexigenic peptide that antagonizes leptin action through the activation of hypothalamic neuropeptide Y/Y1 receptor pathway. Diabetes 50:227–232
13. Tschop M, Smiley DL, Heiman ML 2000 Ghrelin induces adiposity in rodents. Nature 407:908–913
14. Wren AM, Small CJ, Abbott CR, Dhillo WS, Seal LJ, Cohen MA, Batterham RL, Taheri S, Stanley SA, Ghatei MA, Bloom SR 2001 Ghrelin causes hyperphagia and obesity in rats. Diabetes 50:2540–2547
15. Nagaya N, Uematsu M, Kojima M, Ikeda Y, Yoshihara F, Shimizu W, Hosoda H, Hirota Y, Ishida H, Mori H, Kangawa K 2001 Chronic administration of ghrelin improves left ventricular dysfunction and attenuates development of cardiac cachexia in rats with heart failure. Circulation 104:1430–1435
16. Nagaya N, Kangawa K 2003 Ghrelin improves left ventricular dysfunction and cardiac cachexia in heart failure. Curr Opin Pharmacol 3:146–151
17. Enomoto M, Nagaya N, Uematsu M, Okumura H, Nakagawa E, Ono F, Hosoda H, Oya H, Kojima M, Kanmatsuse K, Kangawa K 2003 Cardiovascular and hormonal effects of subcutaneous administration of ghrelin, a novel growth hormone-releasing peptide, in healthy humans. Clin Sci (Lond) 105: 431–435
18. Wortley KE, Anderson KD, Garcia K, Murray JD, Malinova L, Liu R, Moncrieffe M, Thabet K, Cox HJ, Yancopoulos GD, Wiegand SJ, Sleeman MW 2004 Genetic deletion of ghrelin does not decrease food intake but influences metabolic fuel preference. Proc Natl Acad Sci USA 101:8227–8232
19. Hosoda H, Kojima M, Matsuo H, Kangawa K 2000 Purification and characterization of rat des-Gln14-ghrelin, a second endogenous ligand for the growth hormone secretagogue receptor. J Biol Chem 275:21995–22000
20. Hosoda H, Kojima M, Mizushima T, Shimizu S, Kangawa K 2003 Structural divergence of human ghrelin. Identification of multiple ghrelin-derived molecules produced by post-translational processing. J Biol Chem 278:64–70
21. Kaiya H, Kojima M, Hosoda H, Koda A, Yamamoto K, Kitajima Y, Matsumoto M, Minamitake Y, Kikuyama S, Kangawa K 2001 Bullfrog ghrelin is modified by n-octanoic acid at its third threonine residue. J Biol Chem 276: 40441–40448
22. Kaiya H, Van Der Geyten S, Kojima M, Hosoda H, Kitajima Y, Matsumoto M, Geelissen S, Darras VM, Kangawa K 2002 Chicken ghrelin: purification, cDNA cloning, and biological activity. Endocrinology 143:3454–3463
23. Matsumoto M, Hosoda H, Kitajima Y, Morozumi N, Minamitake Y, Tanaka S, Matsuo H, Kojima M, Hayashi Y, Kangawa K 2001 Structure-activity relationship of ghrelin: pharmacological study of ghrelin peptides. Biochem Biophys Res Commun 287:142–146
24. Lee HM, Wang G, Englander EW, Kojima M, Greeley Jr GH 2002 Ghrelin, a new gastrointestinal endocrine peptide that stimulates insulin secretion: enteric distribution, ontogeny, influence of endocrine, and dietary manipulations. Endocrinology 143:185–190
25. Chomczynski P, Sacchi N 1987 Single-step method of RNA isolation by acid guanidinium thiocyanate-phenol-chloroform extraction. Anal Biochem 162: 156–159
26. Hillenkamp F, Karas M 1990 Mass spectrometry of peptides and proteins by matrix-assisted ultraviolet laser desorption/ionization. Methods Enzymol 193: 280–295
27. Greenberger NJ, Skillman TG 1969 Medium-chain triglycerides. N Engl J Med 280:1045–1058
28. Reshef L, Olswang Y, Cassuto H, Blum B, Croniger CM, Kalhan SC, Tilghman SM, Hanson RW 2003 Glyceroneogenesis and the triglyceride/fatty acid cycle. J Biol Chem 278:30413–30416
29. Coleman RA, Lewin TM, Muoio DM 2000 Physiological and nutritional regulation of enzymes of triacylglycerol synthesis. Annu Rev Nutr 20:77–103
30. Eaton S, Bartlett K, Pourfarzam M 1996 Mammalian mitochondrial β-oxidation. Biochem J 320(Pt 2):345–357
31. Solberg HE 1971 Carnitine octanoyltransferase. Evidence for a new enzyme in mitochondria. FEBS Lett 12:134–136
32. Miliar A, Serra D, Casaroli R, Vilaro S, Asins G, Hegardt FG 2001 Developmental changes in carnitine octanoyltransferase gene expression in intestine and liver of suckling rats. Arch Biochem Biophys 385:283–289
33. Murthy MS, Bieber LL 1992 Purification of the medium-chain/long-chain (COT/CPT) carnitine acyltransferase of rat liver microsomes. Protein Expr Purif 3:75–79
34. Hanada K 2003 Serine palmitoyltransferase, a key enzyme of sphingolipid metabolism. Biochim Biophys Acta 1632:16–30
35. Babayan VK 1968 Medium-chain triglycerides—their composition, preparation, and application. J Am Oil Chem Soc 45:23–25
36. Fernando-Warnakulasuriya GJ, Staggers JE, Frost SC, Wells MA 1981 Studies on fat digestion, absorption, and transport in the suckling rat. I. Fatty acid composition and concentrations of major lipid components. J Lipid Res 22: 668–674
37. Gibson RA, Kneebone GM 1981 Fatty acid composition of human colostrum and mature breast milk. Am J Clin Nutr 34:252–257
38. Boersma ER, Offringa PJ, Muskiet FA, Chase WM, Simmons IJ 1991 Vitamin E, lipid fractions, and fatty acid composition of colostrum, transitional milk, and mature milk: an international comparative study. Am J Clin Nutr 53:1197–1204

Endocrinology is published monthly by The Endocrine Society (http://www.endo-society.org), the foremost professional society serving the endocrine community.

Downloaded from endo.endojournals.org on March 19, 2006

Adrenomedullin Enhances Angiogenic Potency of Bone Marrow Transplantation in a Rat Model of Hindlimb Ischemia

Takashi Iwase, MD; Noritoshi Nagaya, MD; Takafumi Fujii, MD; Takefumi Itoh, MD; Hatsue Ishibashi-Ueda, MD; Masakazu Yamagishi, MD; Kunio Miyatake, MD; Toshio Matsumoto, MD; Soichiro Kitamura, MD; Kenji Kangawa, PhD

Background—Previous studies have shown that adrenomedullin (AM) inhibits vascular endothelial cell apoptosis and induces angiogenesis. We investigated whether AM enhances bone marrow cell–induced angiogenesis.

Methods and Results—Immediately after hindlimb ischemia was created, rats were randomized to receive AM infusion plus bone marrow–derived mononuclear cell (MNC) transplantation (AM+MNC group), AM infusion alone (AM group), MNC transplantation alone (MNC group), or vehicle infusion (control group). The laser Doppler perfusion index was significantly higher in the AM and MNC groups than in the control group (0.74 ± 0.11 and 0.69 ± 0.07 versus 0.59 ± 0.07, respectively, $P<0.01$), which suggests the angiogenic potency of AM and MNC. Importantly, improvement in blood perfusion was marked in the AM+MNC group (0.84 ± 0.08). Capillary density was highest in the AM+MNC group, followed by the AM and MNC groups. In vitro, AM inhibited MNC apoptosis, promoted MNC adhesiveness to a human umbilical vein endothelial cell monolayer, and increased the number of MNC-derived endothelial progenitor cells. In vivo, AM administration not only enhanced the differentiation of MNC into endothelial cells but also produced mature vessels that included smooth muscle cells.

Conclusions—A combination of AM infusion and MNC transplantation caused significantly greater improvement in hindlimb ischemia than MNC transplantation alone. This effect may be mediated in part by the angiogenic potency of AM itself and the beneficial effects of AM on the survival, adhesion, and differentiation of transplanted MNCs. (*Circulation*. 2005;111:356-362.)

Key Words: peptides ■ angiogenesis ■ peripheral vascular disease

Peripheral vascular disease is a crucial health issue that affects an estimated 27 million people.[1] Despite recent advances in medical intervention, the symptoms of some patients with critical limb ischemia fail to be controlled. Bone marrow–derived mononuclear cells (MNCs) include a variety of stem and progenitor cells, such as endothelial progenitor cells (EPCs), and contribute to pathological neovascularization.[2] MNC transplantation induces therapeutic angiogenesis in ischemic limb[3,4]; however, some patients fail to respond to this cell therapy. Thus, a novel therapeutic strategy to enhance the angiogenic property of MNCs is desirable.

Adrenomedullin (AM) is a potent vasodilator peptide that was originally isolated from human pheochromocytoma.[5] Previous studies have reported that abnormalities of vascular structure are present in homozygous AM knockout mice.[6,7] A recent study has demonstrated that blood flow recovery in ischemic limb and tumor angiogenesis are substantially impaired in heterozygous AM knockout mice.[8] Furthermore, AM has been shown to inhibit vascular endothelial cell apoptosis and induce angiogenesis through the activation of the phosphatidylinositol 3-kinase (PI3K)/Akt pathway.[9,10] These results suggest that AM is indispensable for modulating angiogenesis and vasculogenesis. When these findings are taken together, combination therapy with MNC transplantation and AM infusion may have additional or synergetic effects on therapeutic angiogenesis for the treatment of severe peripheral vascular disease. Thus, the purposes of the present study were (1) to investigate whether local infusion of AM enhances the angiogenic potency of MNC transplantation in a rat model of hindlimb ischemia and (2) to investigate the effects of AM on the survival, adhesion, and differentiation of transplanted MNCs.

Received June 18, 2004; revision received September 9, 2004; accepted November 3, 2004.

From the Departments of Regenerative Medicine and Tissue Engineering (T. Iwase, N.N., T. Itoh), Cardiac Physiology (T.F.), and Biochemistry (K.K.), National Cardiovascular Center Research Institute, Osaka, Japan; Departments of Internal Medicine (N.N., M.Y., K.M.), Pathology (H.I.-U.), and Cardiovascular Surgery (S.K.), National Cardiovascular Center, Osaka, Japan; and Department of Medicine and Bioregulatory Sciences (T. Iwase, T.M.), University of Tokushima Graduate School of Medicine, Tokushima, Japan.

Reprint requests to Noritoshi Nagaya, MD, Department of Regenerative Medicine and Tissue Engineering, National Cardiovascular Center Research Institute, 5-7-1 Fujishirodai, Suita, Osaka 565-8565, Japan. E-mail nagayann@hsp.ncvc.go.jp

© 2005 American Heart Association, Inc.

Circulation is available at http://www.circulationaha.org

DOI: 10.1161/01.CIR.0000153352.29335.B9

Methods

Animal Model of Hindlimb Ischemia

Male Lewis rats (weight 250 to 275 g; Japan SLC Inc, Hamamatsu, Japan) were used in the present study. The left common iliac artery of each rat was resected under anesthesia with pentobarbital sodium (50 mg/kg). The distal portion of the saphenous artery and all side branches and veins were dissected free and excised. The right hindlimb was kept intact and used as the nonischemic limb. Transplantation of bone marrow–derived MNCs and infusion of AM were performed in 40 rats immediately after hindlimb ischemia was created. This protocol resulted in the creation of 4 groups: (1) AM infusion plus MNC transplantation (AM+MNC group, n=10), (2) AM infusion plus PBS injection (AM group, n=10), (3) vehicle infusion plus MNC transplantation (MNC group, n=10), and (4) vehicle infusion plus PBS injection (control group, n=10). The Animal Care Committee of the National Cardiovascular Center approved this experimental protocol.

MNC Transplantation and AM Infusion

Bone marrow was harvested from the femur and tibia in other male Lewis rats, and MNCs were isolated by Ficoll density gradient centrifugation (Lymphoprep, Nycomed). MNCs (5×10^6 cells per animal) or PBS was injected into the ischemic thigh muscle with a 26-gauge needle at 5 different points. Human recombinant AM (0.01 $\mu g \cdot kg^{-1} \cdot min^{-1}$) or vehicle was administered for 7 days with a mini-osmotic pump (ALZET, Palo Alto) implanted in the left inguinal region.

Assessment of Blood Perfusion

To measure serial blood flow for 3 weeks, we used a laser Doppler perfusion image (LDPI) analyzer (Moor Instrument). After blood flow was scanned twice, the average flow values of the ischemic and nonischemic limbs were calculated by computer-assisted quantification. The LDPI index was determined as the ratio of ischemic to nonischemic hindlimb blood perfusion.[11]

Histological Assessment

Three weeks after MNC transplantation and/or AM infusion, 4 pieces of ischemic tissue from the adductor and semimembranous muscles were obtained and snap-frozen in liquid nitrogen. Frozen tissue sections were stained with alkaline phosphatase by an indoxyl tetrazolium method to detect capillary endothelial cells.[3,11] Five fields were randomly selected to count the number of capillaries. The capillary number adjusted per muscle fiber was used to compare the differences in capillary density among the 4 groups.[3]

Monitoring of Transplanted MNCs in Ischemic Hindlimb Muscle

To examine differentiation of transplanted MNCs, 5×10^6 MNCs labeled with red fluorescent dye (PKH26-GL, Sigma Chemical Co) were transplanted into the ischemic thigh muscle in rats with (n=3) and without (n=3) AM infusion. Three weeks after transplantation, frozen tissue sections from ischemic muscle were incubated with anti-von Willebrand factor antibody (vWF, DAKO), anti-CD31 antibody (BD Pharmingen), and anti-α-smooth muscle actin antibody (α-SMA, DAKO), followed by incubation with Alexa Fluor 633 IgG antibody (Molecular Probes) and FITC-conjugated IgG antibody (BD Pharmingen), respectively. Five high-power fields (40×) of each section were randomly selected to count the number of transplanted MNCs, vWF-positive cells, and α-SMA–positive cells.

In Situ Detection of MNC Apoptosis

PKH26-labeled MNCs (5×10^6 cells per animal) were transplanted into the ischemic muscle in rats with (n=2) and without (n=2) AM infusion. Twenty-four hours after transplantation, apoptosis of transplanted MNCs in ischemic tissue was evaluated by terminal dUTP nick-end labeling (TUNEL) assay (ApopTag Fluorescein kit, Serological Corporation), as reported previously.[12]

In Vitro Apoptosis Assay

The antiapoptotic effect of AM on MNCs was evaluated by TUNEL assay. Human MNCs, isolated from peripheral blood, were plated on 12-well plates (1×10^6 cells per well) and cultured in serum-free medium for 24 hours with control buffer, AM, or AM plus wortmannin, a PI3K inhibitor (50 nmol/L). TUNEL for detection of apoptotic nuclei was performed according to the manufacturer's instructions. MNCs were then mounted in medium that contained 4′,6-diamidino-2-phenylindole (DAPI). Randomly selected microscopic fields (n=10) were evaluated to calculate the ratio of TUNEL-positive cells to total cells.

Adhesion Assay

We evaluated whether AM enhances MNC adhesiveness according to a previously reported method.[13] In brief, human umbilical vein endothelial cells (HUVECs) were cultured to confluence on 6-well plates with or without pretreatment with tumor necrosis factor-α (1 ng/mL). In the absence or presence of AM (10^{-7} mol/L), 1×10^6 MNCs labeled with PKH26 were incubated on an HUVEC monolayer for 24 hours. Nonadherent MNCs were removed, and the number of PKH26-positive cells in each well was counted.

Cell ELISA

Expression of adhesion molecules in HUVECs was measured by cell ELISA, as reported previously.[14] In brief, confluent HUVECs on 96-well plates were treated with AM (10^{-7} mol/L) or control buffer for 4 hours. HUVECs were then incubated with monoclonal mouse antibodies against intercellular adhesion molecule-1 (ICAM-1, R&D Systems) and vascular adhesion molecule-1 (VCAM-1, R&D Systems). A protein detector ELISA kit (KPL) was used to detect bound monoclonal antibodies.

EPC Culture Assay

Culture of EPCs was performed as described previously.[11,15,16] In brief, 2×10^6 MNCs were plated in Medium-199 supplemented with 20% FCS, heparin, and antibiotics on fibronectin-coated 6-well plates. AM (10^{-7} mol/L), human recombinant vascular endothelial growth factor (VEGF; 20 ng/mL), or control buffer was added to each plate. After 7 days of culture, nonadherent cells were removed, and adherent cells were incubated with acetylated LDL labeled with DiI (DiI-acLDL, Biomedical Technologies) and FITC-labeled lectin from ulex europaeus (Sigma). Double-positive cells for DiI-acLDL and FITC-labeled lectin were identified as EPCs.[16] Randomly selected microscopic fields (n=10) were evaluated to count the number of EPCs.

Fluorescence-Activated Cell Sorting Analysis

Fluorescence-activated cell sorting was performed to identify characteristics of adherent cells after 7 days of culture.[16] Cells were incubated for 30 minutes at 4°C with anti-human CD31 antibodies (clone L133.1, Becton Dickinson), anti-human KDR antibodies (clone KDR-1, Sigma), and anti-human VE-cadherin antibodies (clone BV6, Chemicon). Isotype-identical antibodies served as controls. Fluorescence-activated cell sorting analyses were performed with a FACSCalibur flow cytometer and Cell Quest software (BD Biosciences).

Real-Time Polymerase Chain Reaction

Expression of calcitonin receptor-like receptor (CRLR), a receptor for AM, was examined by real-time polymerase chain reaction (PCR). Total RNA was extracted from MNCs, EPCs, and HUVECs with an RNA extraction kit (RNeasy Mini Kit, Qiagen) and converted to cDNA by reverse transcription. Real-time PCR was performed with SYBR green dye (QuantiTect SYBR Green PCR kit, Qiagen) and a Prism 7700 sequence detection system (Applied Biosystems). The PCR primers for CRLR were as follows: sense primer 5′-CATTCAACAAGCAGAAGGCG-3′ and antisense primer 5′-AGCCATCCATCCCAGGTTC-3′. For GAPDH, the primers were as follows: sense primer 5′-CAATGCCTCCTGCACCACCAA-3′ and antisense primer 5′-GAGGCAGGGATGATGTTCTGGA-3′. Levels of CRLR mRNA were normalized to that of

GAPDH mRNA. PCR-amplified products were also electrophoresed on 2% agarose gels to confirm that single bands were amplified.

In Vitro Matrigel Assay

HUVECs (1×10^5 cells) were seeded onto 24-well plates coated with Matrigel (Becton Dickinson) in the presence of the combination of control buffer, AM (10^{-7} mol/L), VEGF (10 ng/mL), or neutralizing antibodies against KDR (2 μg/mL, R&D Systems). After incubation for 18 hours, tube formation area was measured as described previously.[17] The control was defined as 100% tube formation, and the percent increase was calculated for each sample.

Measurements of Cytokines

A total of 1×10^6 MNCs or HUVECs were plated in serum-free medium with or without AM (10^{-7} mol/L) on 12-well plates. After 24-hour incubation, the conditioned medium was collected, and VEGF, basic fibroblast growth factor, and hepatocyte growth factor were measured with enzyme immunoassay kits (R&D Systems).

Migration Assay

Migration assay of smooth muscle cells (SMCs) was performed with Transwell (Coster) 24-well plates composed of a collagen-coated membrane with 8-μm pores. Human aortic SMCs, preincubated with serum-free medium for 24 hours to maintain quiescence, were seeded on the upper chamber at a concentration of 1×10^6 cells/mL. Serum-free medium containing control buffer, AM (10^{-7} mol/L), or AM plus wortmannin (50 nmol/L) was placed in the lower chamber. After incubation for 12 hours, the number of migrated cells was counted in the randomly selected fields (n=5).

Statistical Analysis

All values are expressed as mean±SEM. Student's unpaired t test was used to compare differences between 2 groups. Comparisons of parameters among 3 or 4 groups were made by 1-way ANOVA, followed by Scheffé multiple comparison test. Comparisons of the time course of the LDPI index were made by 2-way ANOVA for repeated measures, followed by Scheffé multiple comparison tests. A probability value <0.05 was considered statistically significant.

Results

Blood Perfusion and Capillary Density

Blood perfusion of the ischemic hindlimb increased modestly but gradually in the AM and MNC groups after treatment (Figure 1A). Interestingly, blood perfusion in the AM+MNC group markedly improved within 2 weeks after treatment and showed further improvement thereafter. The LDPI index was significantly higher in the AM, MNC, and AM+MNC groups than in the control group 3 weeks after surgery (Figure 1B). Importantly, the LDPI index was highest in the AM+MNC group among the 4 groups.

Alkaline phosphatase staining of ischemic muscle showed significant augmentation of neovascularization in the AM, MNC, and AM+MNC groups (Figure 2A). The capillary/muscle fiber ratio of ischemic muscle was highest in the AM+MNC group, followed by the MNC group, AM group, and control group (Figure 2B).

Differentiation of Transplanted MNCs

Three weeks after MNC transplantation, PKH26-labeled MNCs were frequently observed in the AM+MNC group, and these transplanted cells were positive for vWF (Figure 3A). Most of these cells were also stained by CD31 (data not shown). The number of PKH26/vWF double-positive cells was significantly higher in the AM+MNC group than in the MNC group (Figure 3B). Although PKH26/α-SMA double-positive cells were not detected in ischemic muscle of each group, newly formed vascular structures in the AM+MNC group included α-SMA–positive cells (Figure 3C). The number of α-SMA–positive cells in the MNC-derived vascular structures was significantly higher in the AM+MNC group than in the MNC group (Figure 3D).

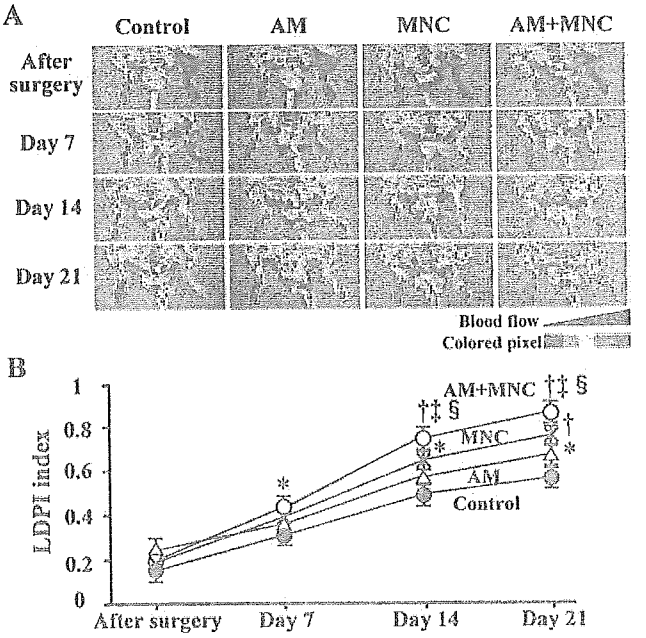

Figure 1. A, Representative examples of serial laser Doppler perfusion images. Blood perfusion of ischemic hindlimb increased notably in AM+MNC group (red to yellow). B, Quantitative analysis of hindlimb blood perfusion with LDPI index, ratio of ischemic to nonischemic hindlimb blood perfusion. Data are mean±SEM. *$P<0.05$ and †$P<0.01$ vs control; ‡$P<0.01$ vs AM; §$P<0.05$ vs MNC.

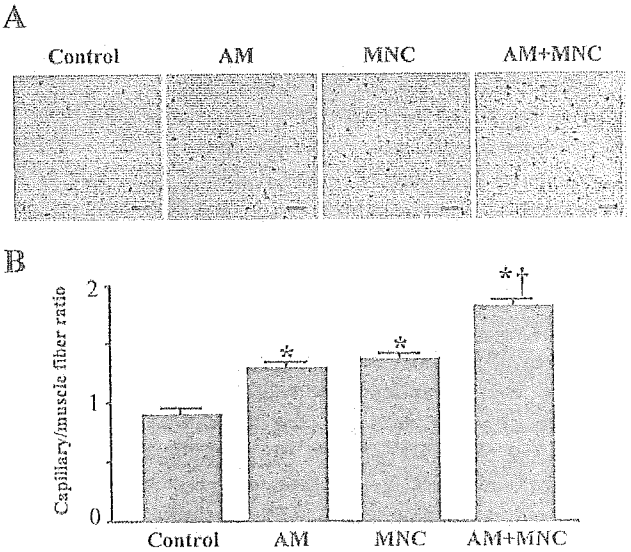

Figure 2. A, Representative photographs of alkaline phosphatase staining in ischemic hindlimb muscles. Capillary density in AM+MNC group was markedly higher than that in other groups. B, Quantitative analysis of capillary density in ischemic hindlimb muscles. Data are mean±SEM. *$P<0.01$ vs control; †$P<0.01$ vs AM and MNC. Scale bars: 50 μm.

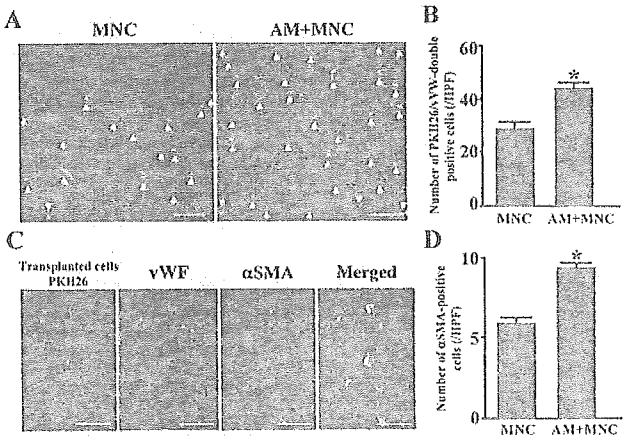

Figure 3. In vivo differentiation of transplanted MNCs. A, Representative photographs of MNC-derived vascular structures in MNC and AM+MNC groups. Red fluorescence (PKH26)–labeled MNCs were transplanted into ischemic thigh muscle. PKH26 (red)/vWF (blue) double-positive cells (pink, arrows) were frequently observed in AM+MNC group. B, Number of PKH26/vWF double-positive cells (MNC-derived endothelial cells) was significantly higher in AM+MNC group than in MNC group. C, Representative photographs of newly formed mature vessels in AM+MNC group. MNC-derived vascular structures often included α-SMA–positive cells (green). D, Number of α-SMA–positive cells in MNC-derived vessels was significantly higher in AM+MNC group than in MNC group. Data are mean±SEM. *$P<0.01$ vs MNC. Bars: 50 μm. HPF indicates high-power field.

Antiapoptotic Effect of AM on MNCs

In vitro, serum starvation induced MNC apoptosis, as indicated by detection of TUNEL-positive cells (Figure 4A). When incubated in the presence of AM, the percentage of TUNEL-positive cells markedly decreased in a dose-dependent manner (Figure 4B). However, pretreatment with wortmannin, a PI3K inhibitor, diminished the antiapoptotic effect of AM. Similarly, in vivo, local administration of AM decreased TUNEL-positive MNC 24 hours after transplantation (data not shown).

Effect of AM on MNC Adhesiveness

The number of adherent MNCs on an HUVEC monolayer increased significantly in the presence of AM (10^{-7} mol/L) compared with control (Figures 5A and 5B). With pretreatment using tumor necrosis factor-α, AM also enhanced the adhesiveness of MNCs to HUVECs. AM significantly enhanced expression of ICAM-1 and VCAM-1 in HUVECs (Figure 5C).

Effect of AM on EPC Expansion

After 7-day culture of human MNCs, spindle-shaped or cobblestone-like adherent cells were observed (Figure 6A). Most of the adherent cells were double stained with DiI-acLDL and FITC-labeled lectin. These adherent cells expressed endothelial cell–specific markers: KDR, VE cadherin, and CD31 (Figure 6B). Thus, we identified the major population of the adherent cells as EPCs. Culture of MNCs with AM significantly increased the number of EPCs (Figure 6C). The effect of AM was equivalent to that of VEGF. Real-time PCR revealed that MNCs, EPCs, and HUVECs expressed mRNA of CRLR (Figure 6D). Expression of

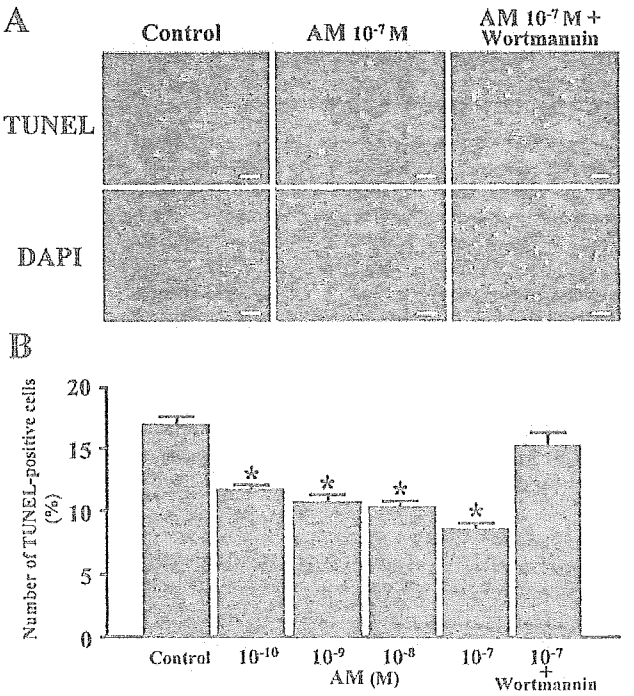

Figure 4. Apoptosis assay. A, Apoptosis of MNC was detected by TUNEL assay (green). Nuclei of MNC were stained with DAPI (blue). AM inhibited MNC apoptosis in serum-free medium. B, Quantitative analysis. AM decreased percentage of TUNEL-positive cells in dose-dependent manner. Pretreatment with wortmannin, a PI3K inhibitor, diminished antiapoptotic effect of AM. Data are mean±SEM. *$P<0.01$ vs control. Bars: 50 μm.

CRLR mRNA was highest in HUVECs, followed by EPCs and MNCs.

Effects of AM on Tube Formation and SMC Migration

Like VEGF, AM induced tube formation in HUVECs in vitro (Figure 7A). Blocking antibodies against KDR significantly inhibited VEGF-induced tube formation, whereas they did not suppress AM-induced tube formation (Figure 7B). AM did not significantly alter VEGF, basic fibroblast growth factor, or hepatocyte growth factor levels in conditioned medium of cultured MNCs or HUVECs (data not shown). AM significantly increased the number of migrated SMCs compared with control (Figures 7C and 7D). Pretreatment with wortmannin diminished the effect of AM on SMC migration.

Discussion

In the present study, we demonstrated in vivo that AM infusion or MNC transplantation alone induced angiogenesis in a rat model of hindlimb ischemia, the combination of AM infusion and MNC transplantation enhanced MNC-induced angiogenesis, and AM increased the number of MNC-derived vWF-positive cells and generated α-SMA–positive vascular structures. We also demonstrated in vitro that AM inhibited serum starvation–induced MNC apoptosis, promoted MNC adhesiveness to an HUVEC monolayer, increased the number of MNC-derived EPCs, and stimulated SMC migration.

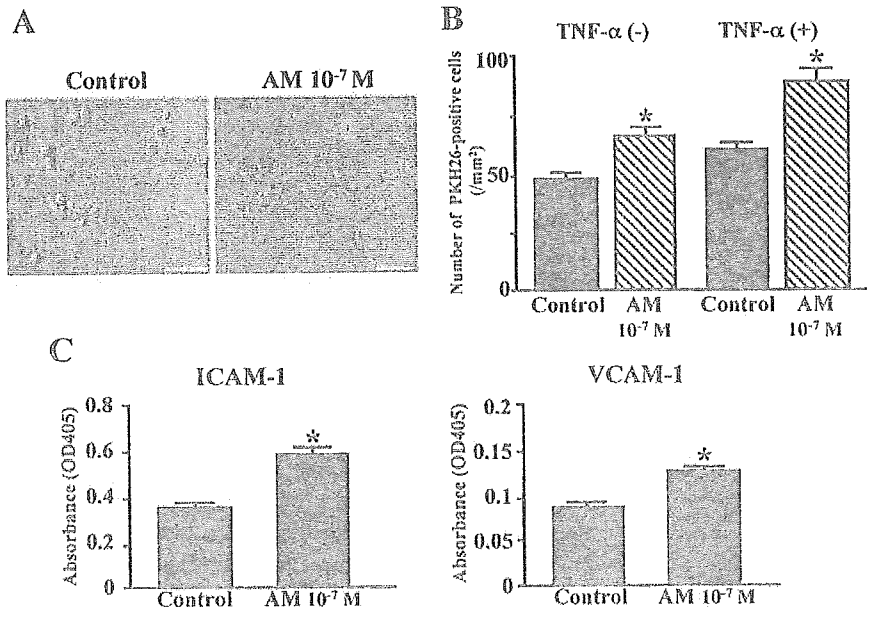

Figure 5. A and B, Adhesion assay. Representative photographs of red fluorescence–labeled MNC adhesion to HUVEC monolayer with and without AM (A). Quantitative analysis of MNC adhesion (B). Bars: 50 μm. C, Surface expression of ICAM-1 and VCAM-1 in HUVECs with or without AM. Data are mean±SEM. TNF indicates tumor necrosis factor. *$P<0.01$ vs control.

MNC transplantation causes therapeutic angiogenesis by supplying EPCs and multiple angiogenic cytokines such as VEGF.[3,4] The present study showed that local infusion of AM significantly increased blood perfusion and capillary density in ischemic hindlimb muscle. Furthermore, a combination of AM infusion and MNC transplantation significantly increased blood perfusion and capillary density of the ischemic hindlimb compared with MNC transplantation alone. AM has been shown to induce angiogenesis in vitro and in vivo through the PI3K/Akt pathway.[10,18] In the present study, AM-induced tube formation was not blocked by neutralizing antibodies against KDR. In addition, AM did not enhance VEGF secretion from MNCs and HUVECs. Thus, beneficial effects of combination therapy

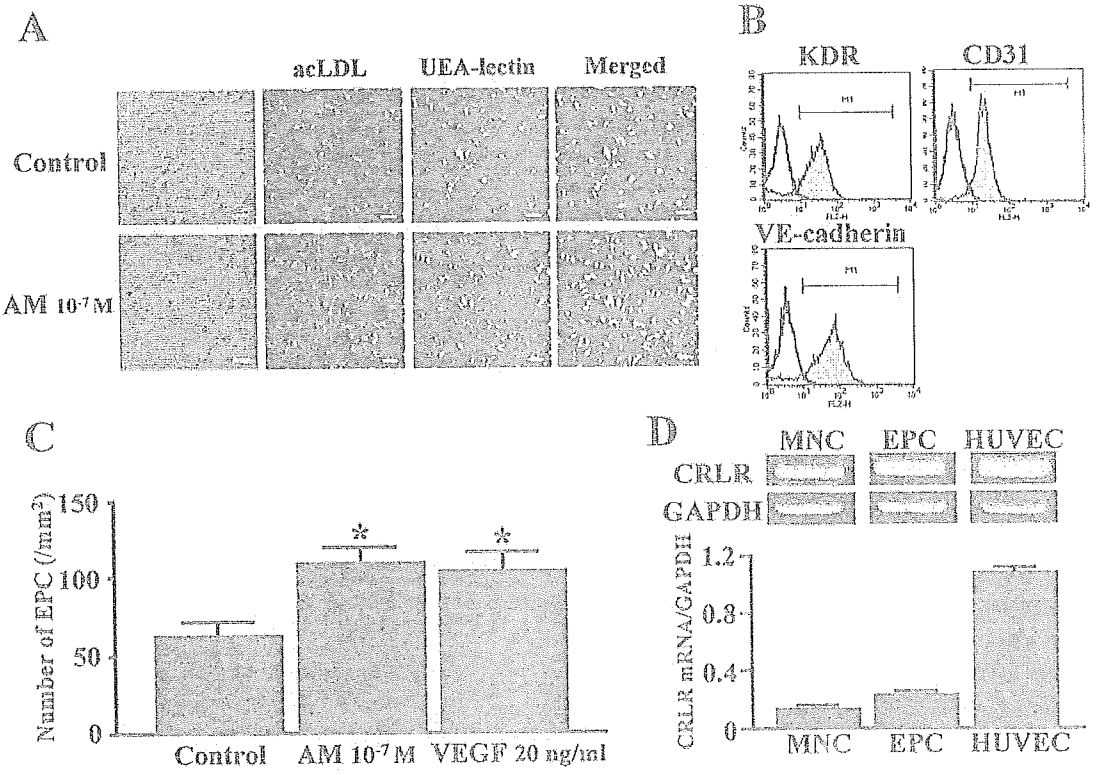

Figure 6. A through C, EPC culture assay. Cultured adherent cells took up DiI-acLDL (red) and FITC-labeled lectin (green) in same fields (A). Fluorescence-activated cell sorting analyses revealed that most adherent cells expressed KDR, VE cadherin, and CD31 (B). Culture of MNCs with AM significantly increased number of EPCs. Effect of AM was equivalent to that of VEGF (C). Data are mean±SEM. *$P<0.01$ vs control. Bars: 50 μm. D, Quantitative analysis of AM receptor (CRLR) mRNA expression in MNCs, EPCs, and HUVECs. UEA indicates ulex europaeus.

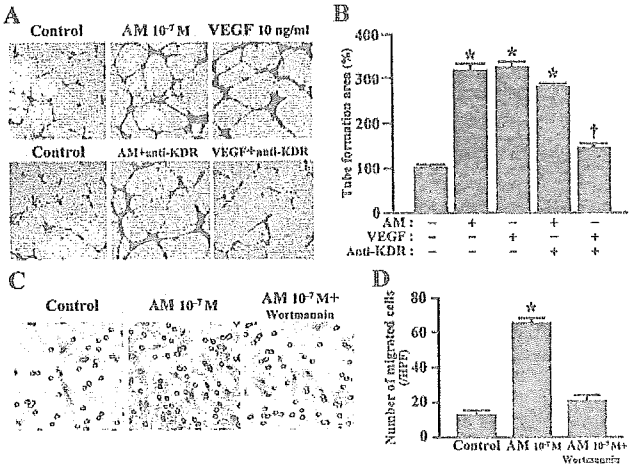

Figure 7. A and B, Matrigel assay. Representative photographs of tube formation (A). Quantitative analysis of tube formation area (B). Data are mean±SEM. *$P<0.01$ vs control; †$P<0.01$ vs VEGF. Bars: 20 μm. C and D, Migration assay. Representative photographs of migrated SMCs (C). Quantitative analyses of SMC migration (D). Data are mean±SEM. *$P<0.01$ vs control. Bars: 50 μm.

with AM and MNCs may be attributable in part to the angiogenic properties of AM itself.

An earlier study has shown that transplanted MNCs disappear from ischemic muscle 7 days after transplantation.[19] We demonstrated that apoptosis of MNCs occurred in ischemic muscle 24 hours after MNC transplantation. These results raise the possibility that the angiogenic potency of MNC transplantation is attenuated by MNC apoptosis. In the present study, AM inhibited apoptosis of MNCs in vitro and in vivo, and the antiapoptotic effect of AM was suppressed by wortmannin, a PI3K inhibitor. These findings suggest that AM prolongs MNC survival through the PI3K/Akt pathway and thereby enhances neovascularization in ischemic tissue.

In the present study, AM promoted adhesiveness of MNCs to an HUVEC monolayer. AM significantly enhanced expression of ICAM-1 and VCAM-1 in HUVECs, both of which facilitate adhesion of MNCs to endothelial cells.[20] These findings suggest that AM increases MNC adhesiveness to endothelial cells via activation of adhesion molecules. A recent study has shown that MNC adhesiveness to endothelial cells is indispensable for MNC differentiation into endothelial lineage.[21] Thus, it is possible that AM infusion enhances the angiogenic potency of MNCs at least in part through promotion of adhesion of MNC to host vascular endothelial cells.

VEGF has been shown to increase the number of EPCs in vitro and in vivo, resulting in angiogenesis and vasculogenesis.[13,22] The present study showed that MNCs and EPCs expressed CRLR, a receptor of AM. In vitro, AM increased the number of MNC-derived EPCs that expressed VE cadherin, KDR, and CD31. The effect of AM on EPC expansion was equivalent to that of VEGF. In vivo, AM infusion increased the number of MNC-derived vWF-positive cells, although incorporation of these cells in the capillaries may be due in part to incorporation of hematopoietic cells. These findings suggest that AM may accelerate MNC differentiation into endothelial lineage.

SMC is essential for the generation of functional and mature blood vessels.[23] We demonstrated in vivo that local infusion of AM increased the number of α-SMA–positive cells (SMCs) in MNC-derived vascular structures. In vitro, AM enhanced SMC migration, which was inhibited by wortmannin, a PI3K inhibitor. Recent studies using homozygous AM knockout mice have suggested that AM is indispensable for vascular morphogenesis.[6,7] When these findings are taken together, it is possible that AM contributes to vessel maturation through enhancement of SMC migration via the PI3K/Akt-dependent pathway.

Currently, a new therapeutic approach to augment the efficacy of MNC transplantation is awaited for the treatment of severe peripheral vascular disease. The present study demonstrated that local infusion of AM enhanced the angiogenic potency of MNC transplantation. In the present study, AM inhibited MNC apoptosis and increased the total number of engrafted cells in ischemic tissue, although this study did not show the effect of AM on specific cell populations of MNCs. In addition, AM promoted cell proliferation, migration, and differentiation. We have already demonstrated the safety of AM infusion in patients with congestive heart failure.[24] Thus, combination therapy with AM infusion and MNC transplantation may be a novel and promising therapeutic strategy for the treatment of severe peripheral vascular disease.

Conclusions

A combination of AM infusion and MNC transplantation caused significantly greater improvement in hindlimb ischemia than MNC transplantation alone. This effect may be mediated in part by the angiogenic potency of AM itself and the beneficial effects of AM on the survival, adhesion, and differentiation of transplanted MNCs.

Acknowledgments

This work was supported by the research grant for cardiovascular disease (16C-6) from the Ministry of Health, Labor and Welfare, Industrial Technology Research Grant Program in '03 from New Energy and Industrial Technology Development Organization (NEDO) of Japan, Health and Labor Sciences Research Grants-genome 005, the Mochida Memorial Foundation for Medical and Pharmaceutical Research, and the Promotion of Fundamental Studies in Health Science of the Organization for Pharmaceutical Safety and Research (OPSR) of Japan.

References

1. Belch JJ, Topol EJ, Agnelli G, et al. Critical issues in peripheral arterial disease detection and management: a call to action. *Arch Intern Med.* 2003;163:884–892.
2. Asahara T, Masuda H, Takahashi T, et al. Bone marrow origin of endothelial progenitor cells responsible for postnatal vasculogenesis in physiological and pathological neovascularization. *Circ Res.* 1999;85:221–228.
3. Shintani S, Murohara T, Ikeda H, et al. Augmentation of postnatal neovascularization with autologous bone marrow transplantation. *Circulation.* 2001;103:897–903.
4. Tateishi-Yuyama E, Matsubara H, Murohara T, et al. Therapeutic angiogenesis for patients with limb ischaemia by autologous transplantation of bone-marrow cells: a pilot study and a randomised controlled trial. *Lancet.* 2002;360:427–435.

5. Kitamura K, Kangawa K, Kawamoto M, et al. Adrenomedullin: a novel hypotensive peptide isolated from human pheochromocytoma. *Biochem Biophys Res Commun.* 1993;192:553–560.
6. Shindo T, Kurihara Y, Nishimatsu H, et al. Vascular abnormalities and elevated blood pressure in mice lacking adrenomedullin gene. *Circulation.* 2001;104:1964–1971.
7. Caron KM, Smithies O. Extreme hydrops fetalis and cardiovascular abnormalities in mice lacking a functional adrenomedullin gene. *Proc Natl Acad Sci U S A.* 2001;98:615–619.
8. Iimuro S, Shindo T, Moriyama N, et al. Angiogenic effects of adrenomedullin in ischemia and tumor growth. *Circ Res.* 2004;95:415–423.
9. Kim W, Moon SO, Sung MJ, et al. Protective effect of adrenomedullin in mannitol-induced apoptosis. *Apoptosis.* 2002;7:527–535.
10. Miyashita K, Itoh H, Sawada N, et al. Adrenomedullin provokes endothelial Akt activation and promotes vascular regeneration both in vitro and in vivo. *FEBS Lett.* 2003;544:86–92.
11. Murohara T, Ikeda H, Duan J, et al. Transplanted cord blood-derived endothelial precursor cells augment postnatal neovascularization. *J Clin Invest.* 2000;105:1527–1536.
12. Okumura H, Nagaya N, Itoh T, et al. Adrenomedullin infusion attenuates myocardial ischemia/reperfusion injury through the phosphatidylinositol 3-kinase/Akt-dependent pathway. *Circulation.* 2004;109:242–248.
13. Iwaguro H, Yamaguchi J, Kalka C, et al. Endothelial progenitor cell vascular endothelial growth factor gene transfer for vascular regeneration. *Circulation.* 2002;105:732–738.
14. Byrne MF, Corcoran PA, Atherton JC, et al. Stimulation of adhesion molecule expression by Helicobacter pylori and increased neutrophil adhesion to human umbilical vein endothelial cells. *FEBS Lett.* 2002;532:411–414.
15. Asahara T, Murohara T, Sullivan A, et al. Isolation of putative progenitor endothelial cells for angiogenesis. *Science.* 1997;275:964–967.
16. Nagaya N, Kangawa K, Kanda M, et al. Hybrid cell-gene therapy for pulmonary hypertension based on phagocytosing action of endothelial progenitor cells. *Circulation.* 2003;108:889–895.
17. Miura S, Matsuo Y, Saku K. Transactivation of KDR/Flk-1 by the B2 receptor induces tube formation in human coronary endothelial cells. *Hypertension.* 2003;41:1118–1123.
18. Tokunaga N, Nagaya N, Shirai M, et al. Adrenomedullin gene transfer induces therapeutic angiogenesis in a rabbit model of chronic hindlimb ischemia: benefits of a novel nonviral vector, gelatin. *Circulation.* 2004;109:526–531.
19. Iba O, Matsubara H, Nozawa Y, et al. Angiogenesis by implantation of peripheral blood mononuclear cells and platelets into ischemic limbs. *Circulation.* 2002;106:2019–2025.
20. Peled A, Grabovsky V, Habler L, et al. The chemokine SDF-1 stimulates integrin-mediated arrest of CD34(+) cells on vascular endothelium under shear flow. *J Clin Invest.* 1999;104:1199–1211.
21. Fujiyama S, Amano K, Uehira K, et al. Bone marrow monocyte lineage cells adhere on injured endothelium in a monocyte chemoattractant protein-1-dependent manner and accelerate reendothelialization as endothelial progenitor cells. *Circ Res.* 2003;93:980–989.
22. Asahara T, Takahashi T, Masuda H, et al. VEGF contributes to postnatal neovascularization by mobilizing bone marrow-derived endothelial progenitor cells. *EMBO J.* 1999;18:3964–3972.
23. Rissanen TT, Markkanen JE, Gruchala M, et al. VEGF-D is the strongest angiogenic and lymphangiogenic effector among VEGFs delivered into skeletal muscle via adenoviruses. *Circ Res.* 2003;92:1098–1106.
24. Nagaya N, Satoh T, Nishikimi T, et al. Hemodynamic, renal, and hormonal effects of adrenomedullin infusion in patients with congestive heart failure. *Circulation.* 2000;101:498–503.